# Kinetic Spectrometry

*with Applications to the Ce-Catalyzed BZ Reaction*

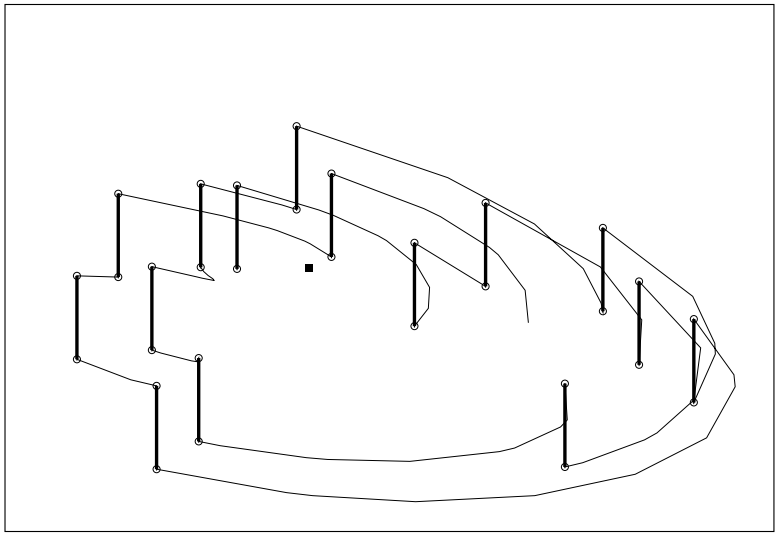

Henrik Skødt

April 1999

*I worked five long years*
*for one woman*
*She had the nerve*
*to kick me out*

-Eddie Boyd, Five Long Years

# Preface

This thesis contains the major part of my work as a master student at chemistry laboratory III at the department of chemistry at the University of Copenhagen. The subject of the thesis is largely due to professor Kenneth Showalter of West Virginia University, who during his stay at chemistry laboratory III during spring of 1998 gave the inspiration to this thesis. His work on control theory laid the foundation, the quenching theory developed at chemistry laboratory III by Preben Graae Sørensen and Finn Hynne provided an aiming point of what should be achieved with the new work.

This leads to the contents of the thesis:

*Chapter one* A general introduction to the subject of oscillating chemical reactions and the contents of the subsequent chapters.

*Chapter two* Specific treatment of the Belousov Zhabotinskii (BZ) reaction, introducing the model used for computer simulations later in the thesis.

*Chapter three* A basic introduction to the algebra necessary to understand the subsequent chapters. It may be skipped by trained readers.

*Chapter four* An introduction to the quenching method and a presentation of previously obtained experimental results for the BZ reaction.

*Chapter five* Treatment of control theory with a notation suited to fit the notation used for Kinetic Spectrometry to emphasize similarities.

*Chapter six* The core of this thesis, Kinetic Spectrometry. A detailed treatment of the theory of the method and connected experiments on the BZ reaction.

*Chapter seven* Conclusions and perspectives on the results of the thesis.

It is my sincere hope that this organization of the chapters together with the layout of the text will provide a continuous and enjoyable reading of the thesis.

At this point it is customary to acknowledge the efforts done by other people, so I will not differ. Naturally, I thank my supervisors, Finn Hynne and Preben Graae Sørensen, for their advice and guidance, and Kenneth Showalter for introducing the opportunity to investigate the possibilities of Kinetic Spectrometry. Morten Hendriksen gave well-placed criticism of the first four chapters, and he made all computer problems disappear like a true magician. Probably the most valuable contribution, though, came from Sune Danø, who almost took the role as a third supervisor at certain times. Not only did he do almost all the Pascal programming for the data interface, he never became tired of discussing small details in the experimental setup or in the theoretical part. Above all I thank him for making it a pleasant thing to share an office with him. B. makes me sing the blues.

Henrik Skødt

Copenhagen, April 1999

# Contents

# 1 Introduction

The immediate attraction of an oscillating chemical reaction is the fact that it oscillates. A sure "eye-catcher" at presentations of the chemistry education at the University of Copenhagen is the ferroin-catalyzed BZ reaction, that changes colour from red to blue and back again. And it keeps on going for a while. The curiosity arises from the common perception, that a chemical reaction consists of reactants that react to produce products, and nothing further.

The phenomenon of oscillating reactions in homogeneous systems and pattern formation in the corresponding non-homogeneous systems is no longer an exotic occurrence that really isn't supposed to happen. Many different reactions have shown oscillations, both simple oscillations with uniform amplitude all the time and more complex oscillations, even chaotic oscillations (see examples in fig. 1.1). By further study one finds the same kind of dynamical behaviour in other scientific disciplines as well, especially physics has many examples of oscillations and pattern formation. The common denominator for all the different disciplines is the mathematics that lies behind the dynamics. The theory for solving and characterizing coupled nonlinear differential equations is at present an active research area for mathematicians, and at least a basic knowledge of this field within mathematics is required to work with oscillating chemical reactions.

Chemical kinetics in solutions provides many examples of nonlinear differential equations, actually the only linear ones are the ones that describe zero and first order kinetics. If there are many different reactions occurring at the same time, some of which have nonlinear rate equations, they can show oscillations in the concentrations of some of the participating species, if they contain a feedback mechanism. Considering a specific reaction this means that one of the products of this reaction must, through other reactions, have an influence on the formation of one of the reactants of the same reac-

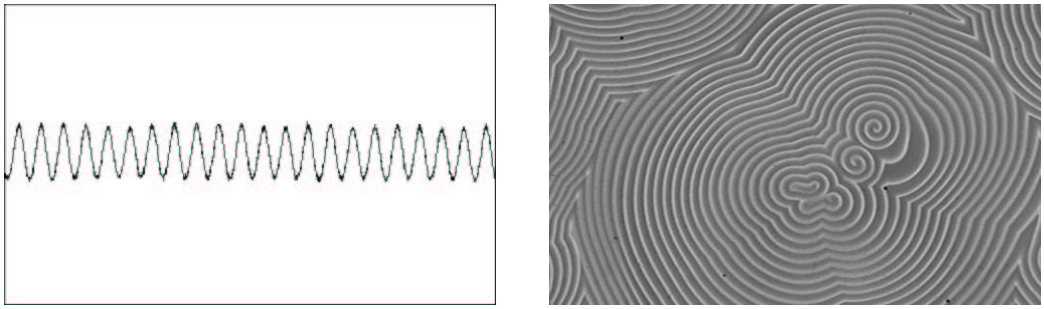

**Figure 1.1**: An example of oscillations in living yeast cells in a stirred system, and spiral patterns in the ruthenium catalyzed BZ reaction (courtesy of Sune Danø and Flemming Jensen).

tion. This will give the coupling between the resulting nonlinear differential equations.

For mathematicians the underlying mathematical theory is in itself interesting. For chemists the incentive is rather the possibility to get chemical information from the mathematics. This is not an easy task, though, because it is rarely possible to measure the concentration of more than one species at a time in a dynamical system. If the chemical mechanism is known, it is relatively easy to find out which dynamical features it contains, compared to watching the dynamics, which does not give away the chemical mechanism. Since the chemical mechanism is the main point of interest for a chemist, it would be nice to have a method to deduce the mechanism from the dynamics. One method that reveals some of the chemistry is the quenching method. Inspired by the quenching method and based on linear control theory, Kinetic Spectrometry is a method that goes a step further. By utilizing the mathematical structures of the chemical reaction it provides a strong tool for estimating whether a proposed mechanism is true or not. The common denominator is the fact that all three methods use measurements of the chemical system's response to perturbations with the participating species. The advantage of Kinetic Spectrometry is that by monitoring only a single species, a maximum amount of information about the mechanism of the reaction can be achieved.

The name Kinetic Spectrometry derives from the way the method is applied to chemical systems. By perturbing the system and measuring the response we can determine the eigenvalues of the kinetics of the chemical system, i.e. we perform spectrometry on the kinetics of the chemical system. This could be compared to Infra-Red spectroscopy for instance. There, perturbing the chemical compound with infrared light reveals the vibrational energy levels of the compound, i.e. the eigenvalues of the Hamiltonian.

# 2 Chemistry of the BZ Reaction

This chapter contains basic information on some of the chemistry involved in the Belousov-Zhabotinskii (BZ) reaction, which has shown all kinds of oscillations in the concentrations of some of the participating species. As stated in the preface this is a chemical thesis, and this chapter focuses on the fact that behind all the algebra in the following chapters lies the seeking of insight into a chemical problem.

## 2.1 The Field-Kőrös-Noyes Mechanism

The BZ reaction is the bromination and oxidation of an organic species in acidic solution by bromate and some metal catalyst. Belousov, who discovered the reaction in 1951 [1], used citric acid as the organic substrate, but today it is more common to use malonic acid as Zhabotinskii did in 1964 [36]. As the metal catalyst the couple $Ce^{3+}/Ce^{4+}$ is the most common, and other examples include $Ru(bpy)_3^{2+}/Ru(bpy)_3^{3+}$ and $Fe(phen)_3^{2+}/Fe(phen)_3^{3+}$ respectively[1].

Focusing on the Ce-catalyzed version with malonic acid as organic species, all modelling originates in the mechanism proposed by Field, Kőrös, and Noyes (FKN) in 1972 (see [3] and table 2.1). The reactions (R1)-(R4) containing Br at different oxidation levels are comparatively well established, and the reactions (R5) and (R6) that include the autocatalytic growth of $HBrO_2$ are also widely recognized. The autocatalytic step, where $HBrO_2$

[1]bpy is short for the bidental ligand 2,2'-bipyridine-N,N', and phen is short for the bidental ligand 1,10-phenantroline.

| | | | |
|---|---|---|---|
| (R1) | $HOBr + Br^- + H^+$ | $\rightleftharpoons$ | $Br_2 + H_2O$ |
| (R2) | $HBrO_2 + Br^- + H^+$ | $\rightarrow$ | $2HOBr$ |
| (R3) | $BrO_3^- + Br^- + 2H^+$ | $\rightarrow$ | $HBrO_2 + HOBr$ |
| (R4) | $2HBrO_2$ | $\rightarrow$ | $BrO_3^- + HOBr + H^+$ |
| (R5) | $BrO_3^- + HBrO_2 + H^+$ | $\rightleftharpoons$ | $2BrO_2\cdot + H_2O$ |
| (R6) | $BrO_2\cdot + Ce^{3+} + H^+$ | $\rightleftharpoons$ | $HBrO_2 + Ce^{4+}$ |
| (R7) | $BrO_2\cdot + Ce^{4+} + H_2O$ | $\rightarrow$ | $BrO_3^- + Ce^{3+} + 2H^+$ |
| (R8) | $Br_2 + MA$ | $\rightarrow$ | $BrMA + Br^- + H^+$ |
| (R9) | $6Ce^{4+} + MA + 2H_2O$ | $\rightarrow$ | $6Ce^{3+} + HCOOH + 2CO_2 + 6H^+$ |
| (R10) | $4Ce^{4+} + BrMA + 2H_2O$ | $\rightarrow$ | $Br^- + 4Ce^{3+} + HCOOH + 2CO_2 + 5H^+$ |

**Table 2.1**: The FKN mechanism. MA and BrMA are $CH_2(COOH)_2$ and $BrCH(COOH)_2$ respectively.

catalyzes its own formation, is seen more clearly by adding (R5) + 2(R6):

$$BrO_3^- + HBrO_2 + 2Ce^{3+} + 3H^+ \quad \rightleftharpoons \quad 2HBrO_2 + 2Ce^{4+} + H_2O \qquad (A)$$

Later studies [2] indicate that the reaction rate of (R7) should be set to zero.

### 2.1.1 The Organic Subset

The reactions (R8)-(R10) involving organic species are not nearly as well established as the rest, and many different organic species have been proposed as intermediaries in newer models involving many more different reactions. It is a fact, though, that $CO_2$ is produced in the reaction, which is seen by the development of bubbles in the reaction. HPLC studies on the reaction of $Ce^{4+}$ and malonic acid exclude the possibility of formic acid, HCOOH, being the main product [5], and they determine 1,1,2,2-ethanetetracarboxylic acid (ETA) as one of the two first stable, intermediate products of the reaction. Further HPLC and $^1H$ NMR studies suggest that monomalonylmalonate (MAMA) is the second of the two first intermediate products [26]. Both of them are most likely formed from unstable radicals, ETA from two alkyl malonyl radicals, $\cdot CH(COOH)_2$, and MAMA from one alkyl malonyl radical and one carboxylato malonyl radical, $\cdot OOCCH_2COOH$.

Electron Spin Resonance (ESR) studies [31] reveal that a malonyl radical is produced immediately after the initial mixing of reactants, and it has a concentration in the order of $10^{-8}$ M. The ESR studies also tell us that the malonyl concentration is oscillating, following the $Ce^{4+}$ oscillations closely;

| | | | |
|---|---|---|---|
| (O1) | $BrO_3^- + Br^-$ | $\xrightarrow{k_1}$ | $HBrO_2$ |
| (O2) | $HBrO_2 + Br^-$ | $\xrightarrow{k_2}$ | P |
| (O3) | $BrO_3^- + HBrO_2$ | $\xrightarrow{k_3}$ | $2HBrO_2 + Ce^{4+}$ |
| (O4) | $2HBrO_2$ | $\xrightarrow{k_4}$ | Q |
| (O5) | $Ce^{4+}$ | $\xrightarrow{k_5}$ | $fBr^-$ |

**Table 2.2**: The Oregonator model. P and Q are arbitrary reaction products.

but they also tell us that the oscillations of $Ce^{4+}$ and $Br^-$ are independent of the malonyl oscillations.

Recent studies [29] of the BZ reaction in a closed system with $^{13}C$ NMR show that there is only one other species besides malonic acid with large enough concentration to appear in the $^{13}C$ spectrum after just 10 minutes. Doing $^{13}C$ NMR under similar circumstances as in [26] shows that neither ETA nor MAMA is the unknown peak. Remembering the result from [31], the unknown peak is most likely the malonyl radical, the precursor to ETA and MAMA. Bromomalonic acid, bromoacetic acid, and dibromoacetic acid are only present in large enough quantities to be measured by $^{13}C$ NMR after the oscillations have been running a while, suggesting that they are products of the reaction, not excluding the possibility of BrMA being important for the behaviour of the oscillations in closed systems by slow build-up of the BrMA-concentration, which has been proposed on several occasions [11, 33, 34].

The problem with the results of the $Ce^{4+}$-malonic acid reaction is that they do not necessarily tell us anything about the intermediates of the BZ reaction, because the analysis has been performed on a reaction that comes to an end. We did not observe the same peaks in the $^{13}C$ NMR of the BZ and $Ce^{4+}$-malonic acid reactions either, suggesting that the two first stable intermediates of the $Ce^{4+}$-malonic acid reaction are never present in the BZ reaction in large quantities.

Whatever mechanism for the organic part of the reaction is correct, the essential feature is the regeneration of bromide ion. Otherwise there can be no oscillations.

## 2.2 The Oregonator Model

The FKN mechanism led to the Oregonator model by Field and Noyes in 1974 (see [4] and table 2.2). The Oregonator is a 3-dimensional model, i.e. it has three dynamical species, $HBrO_2$, $Br^-$, and $Ce^{4+}$, and it captures the essential dynamics of the FKN mechanism. Bromate, although included in

the Oregonator, is not a dynamical species, but the bromate concentration plays the role of an adjustable parameter. None of the reverse reactions are considered in the model, and the $H^+$-concentration is included in the rate constants. It is easy to see the connection, when comparing the Oregonator model with the FKN scheme; e.g. the autocatalytic step, (O3), is clearly the equivalent of reaction (A). The stoichiometric factor, $f$, in (O5) is included, because there is much uncertainty as to how often $Ce^{4+}$ reacts with an organic species via (R9) or via (R10) to produce $Br^-$. Also the Oregonator does not attempt to include any specific organic species due to the uncertainty about which species are actually involved in the organic subset, and the fact that regeneration of $Br^-$ is the most important feature of the organic subset.

In most of the literature, when writing the dynamics of the Oregonator, it is written with symbolic letters for the concentrations of the different species, A for $BrO_3^-$, X for $HBrO_2$, Y for $Br^-$, and Z for $Ce^{4+}$, because it simplifies the appearance of the equations. Using mass action kinetics on the five reactions, (O1)-(O5), results in the following expressions for the reaction velocities of the dynamical species

$$\frac{\mathrm{dX}}{\mathrm{dt}} = k_1\mathrm{AY} - k_2\mathrm{XY} + k_3\mathrm{AX} - 2k_4\mathrm{X}^2 \tag{2.2a}$$

$$\frac{\mathrm{dY}}{\mathrm{dt}} = -k_1\mathrm{AY} - k_2\mathrm{XY} + fk_5\mathrm{Z} \tag{2.2b}$$

$$\frac{\mathrm{dZ}}{\mathrm{dt}} = k_3\mathrm{AX} - k_5\mathrm{Z} \tag{2.2c}$$

where $k_1 - k_5$ are the reaction rate constants.

The complete appearance of the equations furthermore depends on the experimental conditions that the equations are supposed to model. We shall focus on reactions in well-stirred, i.e. homogeneous, systems. If the reaction takes place in a closed system, also known as a batch reactor, the concentration of $BrO_3^-$ will slowly decrease as the reaction proceeds, i.e. the $BrO_3^-$ concentration can not be kept constant in the model. Alternatively the reaction can take place in an open system with constant inflow of reactants, where the experimental setup is known as a Continuous Stirred Tank Reactor (CSTR). Here the $BrO_3^-$ concentration is constant, and to each of the three rate expressions should be added a removal term, e.g. $-j\mathrm{X}$, corresponding to the outflow, where $j$ is the specific flow rate of the system.

For more reading on the BZ reaction and other oscillating chemical systems, [7] and [25] are recommended.

# 3
# Differential Equations and Bifurcations

This chapter gives a basic introduction to the mathematics of nonlinear dynamics, and it is intended to introduce only the concepts necessary to proceed with the following chapters. To many people this chapter will seem very basic indeed, but it is also meant to give people, not trained in nonlinear dynamics, a chance to read this thesis.

## 3.1 Linear Systems

The time evolution of a chemical system is often described by differential equations in the concentrations of the participating chemical species. The set of differential equations that describe the time evolution of the chemical system is referred to as the dynamical system, revealing the fact that they actually do describe something that is time-dependent. A set of differential equations can in general be termed a dynamical system even though the variables may not have any chemical or physical meaning. When one speaks of a linear system, it is a dynamical system that consists of linear differential equations only. In general a linear system can be written as

$$\dot{\mathbf{x}} = \mathbf{A} \cdot \mathbf{x} \tag{3.1}$$

where $\mathbf{x}$ is a real $n$-dimensional vector and $\mathbf{A}$ is a real $n \times n$ matrix. A dot above a symbol is commonly accepted as meaning differentiation with respect to time, i.e. $\dot{\mathbf{x}} = \frac{d\mathbf{x}}{dt}$. In two dimensions, eq. (3.1) gets the appearance

$$\begin{aligned} \dot{x} &= ax + by \\ \dot{y} &= cx + dy \end{aligned}$$

with

$$\mathbf{A} = \begin{pmatrix} a & b \\ c & d \end{pmatrix} \qquad \text{and} \qquad \mathbf{x} = \begin{pmatrix} x \\ y \end{pmatrix}$$

The solution to eq. (3.1) can be proven to be the same in the general $n$-dimensional case as in the 1-dimensional case, i.e.

$$\mathbf{x}(t) = e^{\mathbf{A}t} \cdot \mathbf{x}_0 \tag{3.2}$$

where $e^{\mathbf{A}}$ is defined by its Taylor series,

$$e^{\mathbf{A}} = \sum_{i=0}^{\infty} \frac{\mathbf{A}^i}{i!}$$

and $\mathbf{x}_0$ is the initial condition for $\mathbf{x}(t)$ at $t = 0$. If $n$ linear independent solutions to eq. (3.1) exist, it is possible to write any solution as a linear combination of those. Assuming that $\mathbf{A}$ has $n$ linearly independent eigenvectors, $\mathbf{e}_1, \ldots, \mathbf{e}_n$, with corresponding eigenvalues $\lambda_1, \ldots, \lambda_n$, they are a convenient choice, and the solution is

$$\mathbf{x}(t) = \sum_{i=1}^{n} a_i e^{\lambda_i t} \mathbf{e}_i \tag{3.3}$$

with the coefficients, $a_i$, determined by the initial conditions.

### 3.1.1 Stationary States

The vector, $\mathbf{x}(t)$, is also said to describe the *state* of the system, and the state is stationary when it no longer "moves", i.e. when $\dot{\mathbf{x}} = 0$. For linear systems like (3.1) there is only one stationary solution, the origin. The stability of the stationary state is determined by the real part of the eigenvalues of $\mathbf{A}$.

As an example one could consider a perturbation of the system from the stationary state along $\mathbf{e}_1$, assuming that $\lambda_1$ is real and larger than zero. The system will then move exponentially away from the stationary state along $\mathbf{e}_1$. This is obvious from the fact that in this case

$$\mathbf{x}(t) = a_1 e^{\lambda_1 t} \mathbf{e}_1$$

By the same argument it is obvious that if $\lambda_1$ is real and negative, the same perturbation as before will result in a decay back towards the stationary state along $\mathbf{e}_1$. From eq. (3.3) it can be seen that a random perturbation from the stationary state will result in a motion that is a linear combination of motions along eigenvectors. It is also clear that if just one of the eigenvalues, say $\lambda_1$,

is positive then the result of the perturbation will be a motion away from the stationary state, provided $a_1 \neq 0$.

In the case of complex eigenvalues, $\lambda_i = \bar{\lambda}_{i+1} = \alpha_i + i\beta_i$ (a bar denoting complex conjugation) with corresponding eigenvector $\mathbf{u} + i\mathbf{v}$, the solutions in real vector space can be chosen as

$$\begin{aligned} \mathbf{x}_i &= e^{\alpha_i t}(\cos(\beta_i t)\mathbf{u} - \sin(\beta_i t)\mathbf{v}) \\ \mathbf{x}_{i+1} &= e^{\alpha_i t}(\cos(\beta_i t)\mathbf{u} + \sin(\beta_i t)\mathbf{v}) \end{aligned}$$

which are seen to be elliptical motions with exponentially varying amplitudes. Again the sign of $\alpha_i$ determines whether motion is towards or away from the stationary state.

Eigenvectors corresponding to eigenvalues with negative real part span the linear subspace called the *stable subspace* of the linear system (3.1). Equivalently eigenvectors corresponding to eigenvalues with positive real part span the linear subspace called the *unstable subspace* of the linear system. Thus if just one eigenvector belongs to the unstable subspace, the stationary state is *unstable*, since a small perturbation away from it will not make the system return to the stationary state. If all eigenvectors belong to the stable subspace, any perturbation will make the system return to the stationary state, and the stationary state is *stable*.

For two-dimensional systems with real eigenvalues of opposite sign the origin is called a *saddle-point*, whereas systems with real eigenvalues of the same sign have a stable or an unstable *node* at the origin. In the case of two complex conjugate eigenvalues the system has a *focus* at the origin, stability again determined by the sign of the real part.

For a further study of linear systems and the subjects of zero real part eigenvalues and the corresponding center subspaces, which are left out here, [18] and [30] are recommended.

## 3.2 Nonlinear Systems

As mentioned in chapter 1 the most interesting chemical dynamical systems are all nonlinear. For nonlinear systems (3.1) is replaced by the more general expression

$$\dot{\mathbf{x}} = \mathbf{f}(\mathbf{x}) \tag{3.4}$$

For most chemical systems, except some biochemical systems, $\mathbf{f}(\mathbf{x})$ will consist of polynomials in the $x_i$'s. The Oregonator is a good example of this.

Stationary states are characterized by $\dot{\mathbf{x}} = \mathbf{f}(\mathbf{x}_s) = 0$ as in the linear case, but they are not necessarily located at the origin. Actually this would be

very uninteresting from a chemical point of view, since it corresponds to not mixing any species at all. To make use of the theory in the previous section, we perform the coordinate transformation $\mathbf{u} = \mathbf{x} - \mathbf{x}_s$. Doing this, we immediately realize that $\dot{\mathbf{u}} = \dot{\mathbf{x}} - \dot{\mathbf{x}}_s = \dot{\mathbf{x}} = \mathbf{f}(\mathbf{x})$. The next step is a Taylor expansion from the stationary state (remembering that $\mathbf{u} = \mathbf{x} - \mathbf{x}_s$)

$$\begin{aligned} \dot{\mathbf{u}} &= \mathbf{f}(\mathbf{x}_s) + \mathbf{J} \cdot (\mathbf{x} - \mathbf{x}_s) + \mathbf{M}^2 \cdot (\mathbf{x} - \mathbf{x}_s)(\mathbf{x} - \mathbf{x}_s) + \cdots \\ &= \mathbf{J} \cdot \mathbf{u} + \mathbf{M}^2 \cdot \mathbf{u}\mathbf{u} + \cdots \end{aligned} \tag{3.5}$$

where

$$\begin{aligned} J_{ij} &= \left.\frac{\partial f_i}{\partial x_j}\right|_{\mathbf{x}=\mathbf{x}_s} \\ M^2_{ijk} &= \left.\frac{\partial^2 f_i}{\partial x_j \partial x_k}\right|_{\mathbf{x}=\mathbf{x}_s} \end{aligned}$$

$\mathbf{J}$ is known as the *Jacobian matrix* of $\mathbf{f}$. The Jacobian matrix is especially important for the system when it is close to a stationary state, because then we can apply the linear approximation

$$\dot{\mathbf{u}} \simeq \mathbf{J} \cdot \mathbf{u} \tag{3.6}$$

This equation is similar to eq. (3.1) for linear systems, although it only applies in the neighbourhood around the stationary state. Thus a stationary state can be characterized in the same way as stationary states in linear systems, the eigenvalues of the Jacobian matrix determining the stability. Nonlinear systems can have several stationary states, and for each stationary state there is a separate Jacobian matrix determining the stability.

*Example* To provide an example for later use, we can compute the Jacobian matrix for the Oregonator model symbolically. For this purpose we form the vector

$$\mathbf{c} = \begin{pmatrix} \mathrm{X} \\ \mathrm{Y} \\ \mathrm{Z} \end{pmatrix}$$

in concentration space. Equation (2.2) tells us that (including flow terms)

$$\mathbf{f}(\mathbf{c}) = \begin{pmatrix} k_1\mathrm{AY} - k_2\mathrm{XY} + k_3\mathrm{AX} - 2k_4\mathrm{X}^2 - j\mathrm{X} \\ -k_1\mathrm{AY} - k_2\mathrm{XY} + fk_5\mathrm{Z} - j\mathrm{Y} \\ k_3\mathrm{AX} - k_5\mathrm{Z} - j\mathrm{Z} \end{pmatrix} \tag{3.7}$$

This provides us with the Jacobian matrix

$$\mathbf{J} = \begin{pmatrix} -k_2\mathrm{Y}_s + k_3\mathrm{A} - 4k_4\mathrm{X}_s - j & k_1\mathrm{A} - k_2\mathrm{X}_s & 0 \\ -k_2\mathrm{Y}_s & -k_1\mathrm{A} - k_2\mathrm{X}_s - j & fk_5 \\ k_3\mathrm{A} & 0 & -k_5 - j \end{pmatrix} \tag{3.8}$$

### 3.2.1 Subspaces and Manifolds

Just as eq. (3.6) is an approximation of the general eq. (3.4) close to a stationary state, so are the stable and unstable subspaces of (3.6) only an approximation of the more general stable and unstable manifolds of (3.4). A manifold is a generalized surface of arbitrary dimension. In fact the stable and unstable subspaces in the stationary point are tangent to the stable and unstable manifolds respectively. Thus motion on the stable manifold will be towards the stationary state, while motion on the unstable manifold will be away from the stationary state.

### 3.2.2 Periodic Solutions

Nonlinear dynamical systems can also have periodic solutions, where after one period the same state is achieved again. This is seen as oscillations in chemical systems, e.g. the BZ reaction, and can be expressed mathematically as $\mathbf{x}(t) = \mathbf{x}(t + T)$, $T$ being the period of oscillation. In phase space, e.g. the 3-dimensional concentration space in the case of the Oregonator, the solution must thus describe a closed curve. This curve is called a limit cycle. Examples of a periodic solution of the Oregonator and the associated limit cycle can be seen in fig. 3.1. How limit cycles arise will be explained in section 3.3. For further reading on nonlinear systems, [18] is recommended.

## 3.3 Bifurcations

In dynamical systems there may be a variable parameter, like the bromate concentration or the specific flow rate in the Oregonator. When the value of

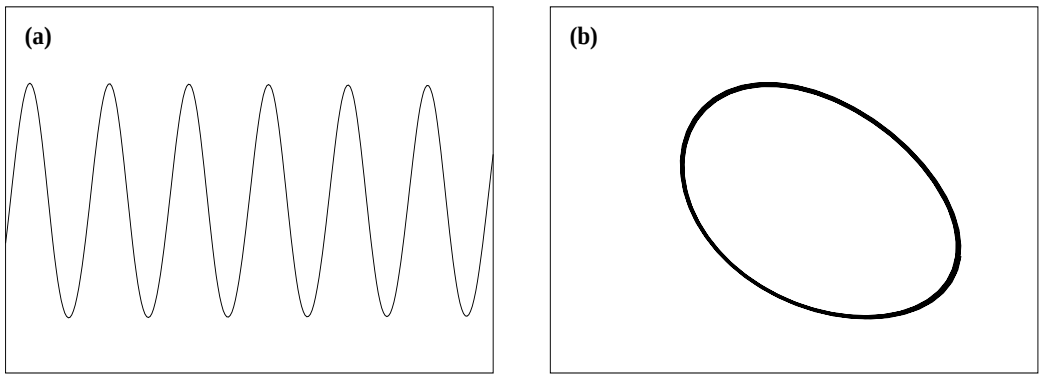


**Figure 3.1**: (a) Oscillations in the $Ce^{4+}$-concentration and (b) the 2D projection of the associated limit cycle on the $[Ce^{4+}]$-$[Br^{-}]$ plane.

this parameter is varied, a significant qualitative change in behaviour of the system may occur. If that is the case, eq. (3.4) is more appropriately written

$$\dot{\mathbf{x}} = \mathbf{f}(\mathbf{x}, \mu) \tag{3.9}$$

where $\mu$ is a real, variable parameter. The value of $\mu$ where the system changes behaviour, $\mu_0$, e.g. a change in stability of a stationary state or periodic solution, is known as the *bifurcation point*. In the strict mathematical sense, this does not come anywhere near a proper definition, but it does give an idea of the concept of bifurcations. To proceed along those lines, it could be useful to illustrate with an example.

*Example* Consider the one-dimensional system

$$\dot{x} = f(x, \mu) = \mu x - x^3$$

For $\mu > 0$ there are three stationary states, $x = 0$ and $x = \pm\sqrt{\mu}$. For $\mu \leq 0$ there is only one stationary state, $x = 0$. To proceed, we calculate $\frac{\partial f}{\partial x} = \mu - 3x^2$. We then insert the stationary state, $x = 0$, and get the one-dimensional Jacobian matrix, $\frac{\partial f}{\partial x}\big|_{x=0} = \mu$, which is identical to the eigenvalue. Thus it is obvious that the stationary state, $x = 0$, is stable for $\mu < 0$ and unstable for $\mu > 0$. Equivalently we get $\frac{\partial f}{\partial x}\big|_{x=\pm\sqrt{\mu}} = -2\mu$ for the stationary states, $x = \pm\sqrt{\mu}$. Thus, they are both stable (since they only exist for $\mu > 0$). For an overview, have a look at the socalled bifurcation diagram in figure 3.2, where $x$ is plotted as a function of $\mu$. This explains the name *pitchfork bifurcation* for this type of bifurcations. In this example, where one stable stationary state changes to an unstable stationary state along with the emergence of two new stable stationary states at $\mu = 0$, the bifurcation point is of course $\mu_0 = 0$.

### 3.3.1 Hopf Bifurcations

Hopf bifurcations have been found in many different physical and chemical, oscillating systems, indeed also in the BZ reaction. Thus it might be

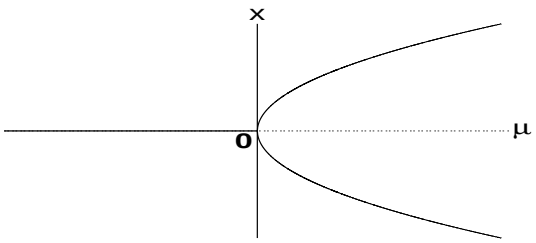


**Figure 3.2**: Bifurcation diagram for the pitchfork bifurcation. The solid lines are the stable stationary states, the dashed line is unstable.

worthwhile to study the characteristics of the Hopf bifurcation.

Consider the $n$-dimensional version of eq. (3.9). Assume that the system has a stationary state, $\mathbf{x}_s$, around the parameter value, $\mu_0$, with eigenvalues $\alpha_i \pm \beta_i$ of the Jacobian matrix. Assume also that the system is "well-behaved", but focusing on chemical systems this should not pose a problem. The following conditions apply for a Hopf bifurcation:

- The Jacobian matrix of (3.9) evaluated at $(\mathbf{x}_s, \mu_0)$ has a pair of complex conjugated, purely imaginary eigenvalues, i.e. $\lambda_i = \bar{\lambda}_{i+1} = i\beta_i$. The remaining $n-2$ eigenvalues should have negative real part.

- The complex pair of eigenvalues crosses the imaginary axis with nonzero speed, i.e.
$$\left.\frac{d\alpha_i(\mu)}{d\mu}\right|_{\mu=\mu_0} \neq 0$$
This condition is known as the *transversality condition*.

- At the bifurcation point emerges a limit cycle, which has zero amplitude.

In practice, in real chemical systems, when observing oscillations in the concentration of one of the participating species, it is impossible to determine whether these conditions are met or not.

First of all it is necessary to distinguish between a supercritical Hopf bifurcation and a subcritical. In the case of a supercritical Hopf bifurcation, the system changes from having a stable focus to having an unstable focus encircled by a stable limit cycle. In the subcritical case, the change goes from unstable focus to stable focus encircled by an unstable limit cycle. Suppose that the bifurcation is supercritical, then it is possible to make the following observations sufficiently close to the bifurcation point:

- The oscillations are nearly sinusoidal, cf. fig. 3.1, and the square of the amplitude of the oscillations can be approximated with a straight line when plotted as a function of the bifurcation parameter [12].

- The period of oscillations, $T$, corresponds to the imaginary part of the eigenvalue, because $\beta_i \approx \frac{2\pi}{T}$. This also applies for the damped oscillations back to the stationary state, that arise if the system is perturbed slightly from the stable focus.

Both the last properties can be derived from the properties of the system on the center manifold associated with the zero real part eigenvalue at the

bifurcation point, but as before all discussion of center manifolds is deliberately skipped. For more in-depth discussion of center manifolds, the center manifold theorem, and Hopf bifurcations in general, the reader is referred to [8], [9], [14], and [18].

*Example* To illuminate the subject further we proceed with another example. Consider the 2-dimensional system

$$\begin{aligned} \dot{x} &= -y + x(\mu - x^2 - y^2) \\ \dot{y} &= x + y(\mu - x^2 - y^2) \end{aligned}$$

It has the eigenvalues $\mu \pm i$ at the stationary state, $(x, y) = (0, 0)$, and thus a Hopf bifurcation at $\mu_0 = 0$. It can be useful to write this system in polar coordinates, $r^2 = x^2 + y^2$ and $\theta = \text{Arctan}(\frac{y}{x})$. With these coordinates, the system becomes

$$\begin{aligned} \dot{r} &= r(\mu - r^2) \\ \dot{\theta} &= 1 \end{aligned}$$

From this it is apparent that the system has a stable circular solution with radius $r = \sqrt{\mu}$, which encircles the unstable stationary state, $r = 0$, that becomes unstable at $\mu = 0$.

Actually the system in the example is a special case of the more general

$$\dot{r} = r(d\mu + ar^2) \tag{3.10a}$$
$$\dot{\theta} = \omega + c\mu + br^2 \tag{3.10b}$$

known as the *Hopf normal form*, where the sign of $a$ determines whether the Hopf bifurcation is supercritical or subcritical. If $a < 0$ then the bifurcation is supercritical, and for $a > 0$ it is subcritical. The criteria with the square of the amplitude of the oscillations forming a straight line when plotted as a function of the bifurcation parameter comes from the fact, that sufficiently close to the bifurcation point a 2D-projection of the $n$-dimensional dynamical system can be approximated by eq. (3.10).

# 4
# Quenching Theory

Quenching theory provides a way of analyzing an oscillating chemical system with a supercritical Hopf bifurcation. In brief it is a perturbation method that uses one perturbation to "quench" the oscillations. This can be done with any of the system's "essential species" or by dilution, and it has been done on a number of different chemical systems [15, 27, 28, 32]. A limitation of the theory is that the quenching has to be performed with the system being close to the Hopf bifurcation, because otherwise the theory does not apply.

## 4.1 The Quenching Equations

Consider an $n$-dimensional oscillating chemical system close to a supercritical Hopf bifurcation. Suppose that we wanted to stop, or quench, the oscillations by making a single perturbation. One solution would be to make a perturbation that shifted the system from the limit cycle to the associated unstable stationary state. This is - in principle - possible, but it would soon prove to be impossible in practice. Especially if one wanted to make the perturbation by addition of only a single species, then it *would* be impossible. Fortunately it is not necessary to hit the stationary state itself but one can aim for the stable manifold of the stationary state instead. A perturbation that hits the stable manifold will make the system move towards the unstable manifold, on which the system moves when oscillating. At the same time the system will start spiralling away from the stable manifold towards the limit cycle, since the stable manifold would have to be hit exactly for the system to stay on it. In real chemical systems that is not possible. In most cases, due to the small real part of the complex eigenvalues, the movement can be perceived as a motion towards the stationary state followed by a spiralling out towards

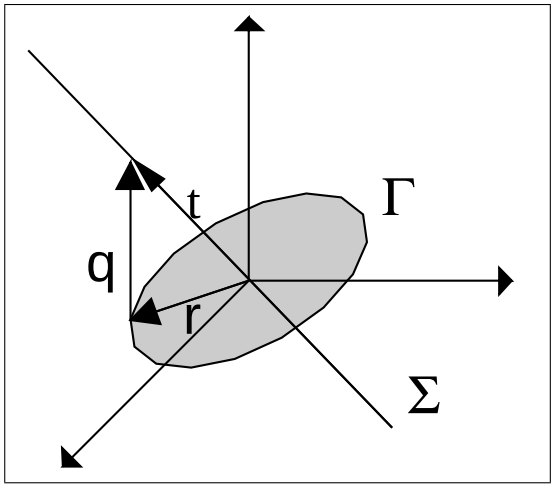


**Figure 4.1**: A quenching with one species, that hits the stable manifold from the limit cycle. The vector $\mathbf{q}$ corresponds to addition of the species whose concentration is along the z-axis. The addition moves the system from the limit cycle, $\mathbf{\Gamma}$ to the stable manifold, $\mathbf{\Sigma}$. The vector $\mathbf{r}$ is a vector from the stationary point to the limit cycle. The vector $\mathbf{t}$ goes from the stationary point to a point on the stable manifold.

the limit cycle. A 3D illustration of a quenching can be seen in fig. 4.1.

### 4.1.1 Quenching by Addition of Single Species

With the designations of fig. 4.1, the quenching vector, $\mathbf{q}$, has to fulfil the property

$$\mathbf{q} = \mathbf{t} - \mathbf{r} \tag{4.1}$$

Since the system is close to a Hopf bifurcation, the motion on the limit cycle can be written as an elliptical motion in the unstable subspace, i.e.

$$\mathbf{r}(t) = \mathbf{u}\cos(\beta t) + \mathbf{v}\sin(\beta t) \tag{4.2}$$

$\mathbf{u}$ and $\mathbf{v}$ are defined as in sec. 3.1, where $\mathbf{e}_1 = \bar{\mathbf{e}}_2 = \mathbf{u} + i\mathbf{v}$ are the eigenvectors corresponding to the complex eigenvalues. The eigenvectors, $\mathbf{e}_i$, of the Jacobian matrix are also known as the *right* eigenvectors of the Jacobian matrix. Alternatively the *left* eigenvectors of the Jacobian matrix, $\mathbf{e}^i$ are defined by $\mathbf{e}^i \cdot \mathbf{J} = \lambda_i \mathbf{e}^i$, and thus we can define the orthonormality of the eigenvectors as

$$\mathbf{e}^j \cdot \mathbf{e}_i = \begin{cases} 1 & \text{for} \quad j = i \\ 0 & \text{for} \quad j \neq i \end{cases} \tag{4.3}$$

For $\mathbf{e}^1$ and $\mathbf{e}^2$ we can write $\mathbf{e}^1 = \bar{\mathbf{e}}^2 = \mathbf{l} + i\mathbf{m}$.

When speaking of performing a quenching, and thus a quenching amplitude and phase, we need to have some reference point. In the case of the BZ reaction, the choice is usually the amplitude of the $Ce^{4+}$-oscillations, and the phase is relative to the maximum of the oscillations. Quenching by addition of the $k$-th species with relative quenching amplitude, $q_k$, and relative phase,

$\phi_k$, can be shown [10] to result in

$$l_k = \frac{-\cos(\phi_k)}{q_k} \tag{4.4a}$$

$$m_k = \frac{-\sin(\phi_k)}{q_k} \tag{4.4b}$$

for the $k$-th component of $\mathbf{l}$ and $\mathbf{m}$. Thus as a consequence, $\mathbf{l}$ and $\mathbf{m}$ can be determined from $n$ independent quenchings. Obviously, $\mathbf{e}^1$ and $\mathbf{e}^2$ are then known also. From the orthonormality condition, (4.3), we get two equations for the determination of $\mathbf{e}_1$ (and consequently $\mathbf{e}_2$):

$$\mathbf{e}^1 \cdot \mathbf{e}_1 = 1 \tag{4.5a}$$

$$\mathbf{e}^2 \cdot \mathbf{e}_1 = 0 \tag{4.5b}$$

These lead to the corresponding equations for $\mathbf{u}$ and $\mathbf{v}$:

$$\mathbf{l} \cdot \mathbf{u} = \frac{1}{2} \tag{4.6a}$$

$$\mathbf{m} \cdot \mathbf{u} = 0 \tag{4.6b}$$

and

$$\mathbf{l} \cdot \mathbf{v} = 0 \tag{4.7a}$$

$$\mathbf{m} \cdot \mathbf{v} = -\frac{1}{2} \tag{4.7b}$$

Still we need to determine $n$ - 2 coordinates of both $\mathbf{e}_1$ and $\mathbf{e}_2$. From eq. (4.2) we get for the relative amplitude, $a_i$, and the relative phase, $\theta_i$, of the $i$-th species:

$$a_i = \sqrt{u_i^2 + v_i^2} \tag{4.8a}$$

$$\theta_i = \mathrm{Arctan}(\frac{v_i}{u_i}) \tag{4.8b}$$

This tells us that if we can monitor $n$ - 2 species and hence obtain their relative amplitudes and phases, then we can determine $\mathbf{e}_1$ and $\mathbf{e}_2$.

### 4.1.2 Quenching by Dilution

Quenching by dilution can be used to find the concentrations of the species in the unstable stationary state, $\mathbf{c}_s$. When quenching the oscillations by dilution, the quenching vector must be $-d\mathbf{c}$, where $d$ is the relative dilution

and $\mathbf{c}$ the concentration vector at the instant of perturbation, since a dilution reduces all concentrations by the same relative amount in the opposite direction of the present concentration vector. Again it is necessary to monitor the concentrations of $n-2$ species, and it can be shown [10] that we get the following equations for the stationary concentrations:

$$-d\mathbf{e}^1 \cdot \mathbf{c} = (d-1)\cos(\phi_d) \tag{4.9a}$$

$$-d\mathbf{e}^2 \cdot \mathbf{c} = (d-1)\sin(\phi_d) \tag{4.9b}$$

We use $\phi_d$ for the relative phase. The stationary concentration found by this method, however, is in fact the average concentration of the species during one cycle. This is not necessarily the same as the stationary concentration, unless the limit cycle is strictly elliptical, which is an approximation, although a good one.

## 4.2 The Quenching Experiments

In the BZ reaction it is possible to measure the concentration of two species simultaneously, i.e. $Ce^{4+}$ by absorption of light and $Br^-$ by bromide-sensitive electrodes. It can be difficult, though, to measure both simultaneously with the adequate accuracy. Assuming that the system is 3-dimensional like the Oregonator solves this problem, because it only requires measuring one species.

Sørensen and Hynne found that the BZ reaction has a supercritical Hopf bifurcation [27]. They worked with a CSTR with three different flows. The first flow was 0.0360 M $KBrO_3$ in 1 M $H_2SO_4$, the second 0.501 M $CH_2(COOH)_2$ and 0.000249 M $Ce_2(SO_4)_3$ in 1 M $H_2SO_4$, and the third 1 M $H_2SO_4$, all with the same flow rate. At 30.0° C they found that the system has a supercritical Hopf bifurcation at the specific flow rate, $j = 3.39 \times 10^{-5}\,\mathrm{s}^{-1}$. They chose to work at a specific flow rate of $5.08 \times 10^{-5}\,\mathrm{s}^{-1}$, which is well within the area where the square of the amplitude of the oscillations forms a straight line as a function of the specific flow rate [12]. Thus they could apply the quenching equations from the previous section. The results of the quenchings with $Ce^{4+}$, $HBrO_2$, and $Br^-$ respectively can be seen in table 4.1. They also performed a quenching by dilution, but did not get a credible

| Addition of | $q_k$ | $\phi_k$, deg. |
|---|---|---|
| $Ce^{4+}$ | 0.43 | -128 |
| $HBrO_2$ | 0.20 | 92 |
| $Br^-$ | 0.110 | -104 |

**Table 4.1**: Results of the quenching experiments. $q_k$ and $\phi_k$ are relative to the amplitude, and the maximum of the $Ce^{4+}$-oscillations, respectively.

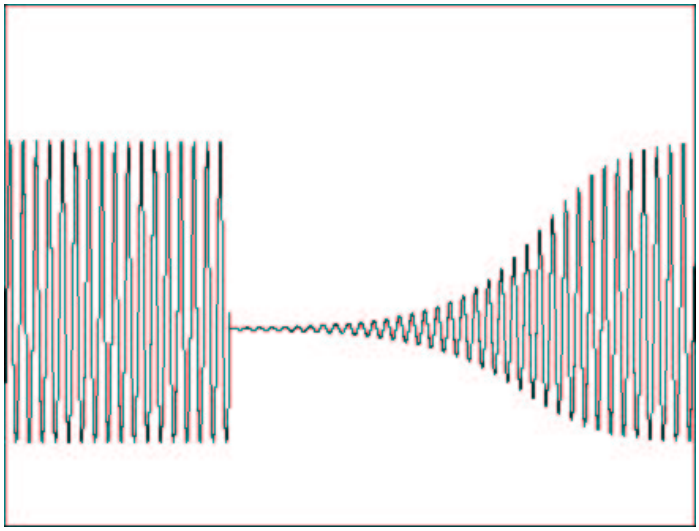

**Figure 4.2**: An example of a quenching performed by addition of $Ce^{4+}$ in a simulation with the Oregonator model.

result. To demonstrate the appearance of a quenching in an experiment, a simulation of a quenching by addition of $Ce^{4+}$ in the Oregonator is shown in fig. 4.2.

With the relative amplitude, $a_{Ce^{4+}} = 1$, and the relative phase, $\theta_{Ce^{4+}} = 0$, of $Ce^{4+}$, we can calculate:

$$u_{Ce^{4+}} = 1 \qquad \text{and} \qquad v_{Ce^{4+}} = 0$$

This together with the results of table 4.1 can be used in eqs. (4.6) and (4.7) to give (in descending order $Ce^{4+}$, $HBrO_2$, and $Br^-$).

$$\mathbf{u} = \begin{pmatrix} 1 \\ -0.33 \\ -0.40 \end{pmatrix} \qquad \text{and} \qquad \mathbf{v} = \begin{pmatrix} 0 \\ -0.088 \\ -0.0070 \end{pmatrix} \tag{4.10}$$

This result is different from the result obtained in [27] because of the different normalization used here, but it is preferred here to be in accordance with the normalization used in Kinetic Spectrometry. Because the system is only 3-dimensional it is also possible to obtain the third *right* eigenvector of the Jacobian matrix, $\mathbf{e}_3$, corresponding to the real, negative eigenvalue. Deciding on 1 as the first coordinate of $\mathbf{e}_3$, the orthonormalization (4.3) gives us

$$\mathbf{e}_3 = \begin{pmatrix} 1 \\ -0.69 \\ -0.60 \end{pmatrix} \tag{4.11}$$

which is, of course, the same result as in [27], since the difference in normalization only affects the complex eigenvectors.

As remarked at the beginning of this chapter, the method only applies close to a Hopf bifurcation, and the closer to the bifurcation, the easier it is to determine the quenching parameters, since it means a longer recovery time from the quenching. Further away from the bifurcation point, due to the larger real part of the complex eigenvalues, the recovery of the oscillations is quite fast, and it can be difficult to determine the correct quenching parameters. This is by no means easy closer to the bifurcation point, and the choice of flow parameter must be a compromise between getting sufficiently close to the bifurcation point and the oscillations being large enough to measure experimentally.

The advantage of the quenching method once a Hopf bifurcation has been found for the chemical system is that it is quite robust, and that it is relatively easy to perform. The backdraw being that a Hopf bifurcation *must* be found, and that it is necessary to monitor $n - 2$ species. However, the quenching method does give some insight into the secrets of the chemical system.

# 5
# Control Theory

Control theory is an old discipline within engineering where it has been used for optimizing yields in different productions etc. The principle is quite simple. By measuring a quantity of the physical system in question (output) it is possible to determine what input to give the system in order to achieve the desired output.

It was not until 1990 that control theory was used on oscillating dynamical systems. Ott, Grebogi, and Yorke devised a simple map-based algorithm (OGY) for stabilizing an unstable limit cycle in a chaotic system [16]. Since then, many people have extended the theory to different parts of the many different kinds of dynamical systems, also to chemical dynamical systems [17, 19, 20, 21].

## 5.1 Linear Control

The first examples of control on chemical systems were conducted with slight modifications of the OGY method, based on one-dimensional mappings. They were applied to chaotic systems, and were successful in stabilizing different periodic oscillations, period-1, period-2, etc. There were, however, limitations of the method, and in this context the autoregressive method based on time series measurements [21] is more interesting, as well as being more generally applicable.

The autoregressive control method can be divided into two parts. The first part is called identification, and in the identification part the coefficients for the second part, the control part, are determined by applying random perturbations to the system and measuring the response. In the control part the previously determined coefficients are used to stabilize an otherwise unstable stationary state of the system by calculating the controlling perturbations

from the identification coefficients. This will be done by assigning stable eigenvalues to the controlled system, the socalled pole-placement technique.

### 5.1.1 Identification

In chapter 3 we saw that the kinetic equations for a homogeneous chemical system consisting of $n$ different chemical dynamical species can be written as

$$\dot{\mathbf{c}} = \mathbf{f}(\mathbf{c})$$

where $\mathbf{c}$ is the $n$-dimensional, time dependent, concentration vector. Assuming that the dynamical system has a stationary state, $\mathbf{c}_s$ (with $\mathbf{f}(\mathbf{c}_s) = \mathbf{0}$), the linear description of the system is

$$\dot{\mathbf{u}} = \mathbf{J} \cdot \mathbf{u}$$

where $\mathbf{u} = \mathbf{c} - \mathbf{c}_s$. The Jacobian matrix, $\mathbf{J}$, is defined as in chapter 3, and its elements express the change of reaction-velocity of the i'th species due to changes in the concentration of the j'th species.

The solution to the linear equation is given in eq. (3.2), and considering $\mathbf{u}$ at a *discrete* set of moments, $t_k$, it becomes

$$\mathbf{u}_k = \mathbf{F} \cdot \mathbf{u}_{k-1} \qquad \text{with} \qquad \mathbf{F} = e^{\mathbf{J}(t_k - t_{k-1})}$$

$\mathbf{F}$ is defined by its Taylor-series, and it has the same eigenvectors as $\mathbf{J}$ with eigenvalues $\rho_i = e^{\lambda_i(t_k - t_{k-1})}$, where $\lambda_i$ are the eigenvalues of $\mathbf{J}$.

For identification of the system it is necessary to perform a number of perturbations to probe the system. These perturbations can both be perturbations of bifurcation parameters, and additions of chemical species. Choosing addition of chemical species, a perturbation will be represented by a vector in concentration space, which will have the same direction on each perturbation, assuming that the additions are taken from the same solution. If the amount of solution added to the system at $t_k$ is called $w_k$, and the direction of the perturbation is represented by the vector, $\mathbf{g}$, then the perturbation at $t_k$ corresponds to adding the term $\mathbf{g}w_k$ to $\mathbf{u}_k$, since by definition the addition of species at $t_k$ can not influence $\mathbf{u}_k$. Keeping $\Delta t = (t_k - t_{k-1})$ constant results in

$$\begin{aligned} \mathbf{u}_k &= \mathbf{F} \cdot (\mathbf{u}_{k-1} + \mathbf{g}w_{k-1}) \\ &= \mathbf{F} \cdot \mathbf{u}_{k-1} + \mathbf{F} \cdot \mathbf{g}w_{k-1} \end{aligned} \tag{5.1}$$

It has been shown that equation (5.1) can be transformed by a similarity transformation to what is known as the canonical form [35]:

$$\mathbf{v}_k = \mathbf{L} \cdot \mathbf{v}_{k-1} + \mathbf{d}w_{k-1} \tag{5.2}$$

where

$$\begin{aligned}
\mathbf{v} &= \mathbf{A}\cdot\mathbf{u} \\
\mathbf{L} &= \mathbf{A}\cdot\mathbf{F}\cdot\mathbf{A}^{-1} = \begin{pmatrix} 0 & 1 & 0 & \cdots & 0 \\ 0 & 0 & 1 & \cdots & 0 \\ \vdots & \vdots & \vdots & \ddots & \vdots \\ 0 & 0 & 0 & \cdots & 1 \\ L_{n1} & L_{n2} & L_{n3} & \cdots & L_{nn} \end{pmatrix} \\
\mathbf{d} &= \mathbf{A}\cdot\mathbf{F}\cdot\mathbf{g}
\end{aligned} \tag{5.3}$$

Consider the quantity $x = \mathbf{h}^{\mathbf{T}}\cdot\mathbf{u}$, $\mathbf{h}$ being an "observation" vector determined from experimental circumstances. This means that $x$ is some linear function of the concentrations of the dynamical species, e.g. $x$ could be absorption measurements of light through a CSTR, the extinction coefficients determining $\mathbf{h}$. It is not necessary to know the function explicitly. We now assume that the $x$'s at different $t_k$'s fulfil an autoregression equation that includes perturbation terms:

$$\begin{aligned}
x_k &= a_1x_{k-1} + a_2x_{k-2} + \cdots + a_nx_{k-n} + \\
&\quad b_1w_{k-1} + b_2w_{k-2} + \cdots + b_nw_{k-n}
\end{aligned} \tag{5.4}$$

The term autoregression is derived from the dependence of $x_k$ on past $x$'s. In real chemical systems it could be impossible to get direct measurements of the deviation from the stationary state, $x$. Usually we can make measurements of absolute values of the system, $y$, and if we assume that the deviation from the value in the stationary state is not too large, we can assume $y = \mathbf{h}^{\mathbf{T}}\cdot\mathbf{c}$ also. The autoregression equation for the $y$'s gets the appearance:

$$\begin{aligned}
y_k &= a_1y_{k-1} + a_2y_{k-2} + \cdots + a_ny_{k-n} + b_0 + \\
&\quad b_1w_{k-1} + b_2w_{k-2} + \cdots + b_nw_{k-n}
\end{aligned} \tag{5.5}$$

Unlike [21] we must require the same indexing of the perturbations as in eq. (5.1). Equation (5.5) also provides the connection between $b_0$ and $\mathbf{c}_s$, since $\mathbf{u} = \mathbf{c} - \mathbf{c}_s$:

$$b_0 = (1 - a_1 - \cdots - a_n)\mathbf{h}^{\mathbf{T}}\cdot\mathbf{c}_s \tag{5.6}$$

It can be shown [13] that the connection between eq. (5.2) and eq. (5.5) is given by the matrix components of eq. (5.3) and the $a$-coefficients of the autoregression equation:

$$L_{n1} = a_n, L_{n2} = a_{n-1}, \ldots, L_{nn} = a_1 \tag{5.7}$$

For the determination of the $2n+1$ coefficients we need in principle $3n+1$ measurements, but in practice it is usually necessary to perform many more measurements to get an overdetermination of the coefficients. To expand on this, consider the ideal case with $3n+1$ measurements. Finding the coefficients corresponds to solving the linear equation

$$\begin{pmatrix} y_k & \cdots & y_{k-n+1} & 1 & w_k & \cdots & w_{k-n+1} \\ y_{k-1} & \cdots & y_{k-n} & 1 & w_{k-1} & \cdots & w_{k-n} \\ \vdots & & \vdots & \vdots & \vdots & & \vdots \\ y_{k-2n} & \cdots & y_{k-3n+1} & 1 & w_{k-2n} & \cdots & w_{k-3n+1} \end{pmatrix} \cdot \begin{pmatrix} a_1 \\ \vdots \\ a_n \\ b_0 \\ b_1 \\ \vdots \\ b_n \end{pmatrix} = \begin{pmatrix} y_{k+1} \\ \vdots \\ y_{k-2n+1} \end{pmatrix}$$

If more than $3n+1$ measurements are required, there will be more equations than unknowns. In that case, the method of Singular Value Decomposition (SVD) is ideal for solving the system of linear equations [24].

To get a proper determination of the coefficients, the perturbations must be chosen in a random manner to avoid degeneracies between columns in the $y, w$-matrix. This can be done in two ways. The first choice is to make perturbations at each $t_k$ but with different $w_k$ every time, i.e. a pseudo-random size perturbation. The other choice is to make the same size perturbation every time, but only to make them at pseudo-random $t_k$'s, e.g. to let $w_k$ be equal to zero except at $t_k$'s with $\frac{t_k}{\Delta t}$ multipla of 7, 13 or 17. The last choice is easier to implement in experiments.

Once the coefficients have been determined, it is worth noticing that we then know the eigenvalues of the autonomous system, i.e. the system without perturbations. Performing a similarity transformation on a matrix does not change its eigenvalues [35], and this means that the eigenvalues of $\mathbf{L}$ are the same as the eigenvalues of $\mathbf{F}$.

The conditions for choosing $\mathbf{h}, \mathbf{g}$ and $\Delta t$ are described in section 6.1.2.

### 5.1.2 Control

Another way of realizing that the $a$-coefficients reveal the eigenvalues of the autonomous system is to consider eq. (5.4), which without perturbations would become

$$\begin{aligned} 0 &= -x_k + a_1 x_{k-1} + \cdots + a_n x_{k-n} \\ &= (-\rho^n + a_1 \rho^{n-1} + \cdots + a_{n-1}\rho + a_n) x_{k-n} \end{aligned} \tag{5.8}$$

showing that the characteristic equation of the matrix $\mathbf{L}$ gives the eigenvalues of the autonomous system.

Including the perturbations in the description of the system can be viewed as changing the dimension of the system from $n$ to $2n$. Consider the autoregression equation (5.4). It shows that if the perturbations are considered variables, the dimension of the system is $2n$. In order to find the eigenvalues of the $2n$-dimensional system we must determine an expression similar to eq. (5.8) for the perturbed system, i.e. we assume that we know the coefficients, $l$, in the expression

$$\begin{aligned} 0 &= -x_k + l_1 x_{k-1} + \cdots + l_{2n} x_{k-2n} \\ &= (-{\rho^*}^{2n} + l_1 {\rho^*}^{2n-1} + \cdots + l_{2n-1}\rho^* + l_{2n}) x_{k-2n} \end{aligned} \tag{5.9}$$

where $\rho^*$ are the eigenvalues of the perturbed system.

To obtain control of the system, the perturbation, $w_k$, must depend on $2n-1$ variables of the system, starting with the index $k-1$. To express it mathematically the equation for $w_k$ becomes

$$\begin{aligned} w_k &= q_1 x_{k-1} + q_2 x_{k-2} + \cdots + q_n x_{k-n+1} + \\ &\quad r_1 w_{k-1} + \cdots + r_{n-1} w_{k-n+2} \end{aligned} \tag{5.10}$$

It can be shown [6] that the expression connecting the $l$-coefficients and the $q, r$-coefficients is

$$\begin{pmatrix} a_1 & -1 & 0 & \cdots & 0 & 0 & \cdots & & & 0 \\ a_2 & a_1 & -1 & \cdots & 0 & b_1 & 0 & \cdots & & 0 \\ a_3 & a_2 & a_1 & \ddots & \vdots & b_2 & b_1 & 0 & \cdots & 0 \\ \vdots & \vdots & \vdots & \ddots & -1 & \vdots & \vdots & \ddots & & \vdots \\ a_n & a_{n-1} & a_{n-2} & \cdots & a_1 & b_{n-1} & b_{n-2} & \cdots & b_1 & 0 \\ 0 & a_n & a_{n-1} & \cdots & a_2 & b_n & b_{n-1} & b_{n-2} & \cdots & b_1 \\ 0 & 0 & a_n & \cdots & a_3 & 0 & b_n & b_{n-1} & \cdots & b_2 \\ \vdots & & \ddots & \ddots & \vdots & \vdots & \ddots & \ddots & \ddots & \vdots \\ 0 & 0 & \cdots & 0 & a_n & 0 & \cdots & 0 & b_n & b_{n-1} \\ 0 & 0 & 0 & \cdots & 0 & 0 & 0 & \cdots & 0 & b_n \end{pmatrix} \cdot \begin{pmatrix} 1 \\ -r_1 \\ \vdots \\ -r_{n-1} \\ q_1 \\ \vdots \\ q_n \end{pmatrix} = \begin{pmatrix} l_1 \\ l_2 \\ \vdots \\ \vdots \\ l_{2n} \end{pmatrix} \tag{5.11}$$

The idea of the pole placement technique is then the following: We choose the eigenvalues of the perturbed system to have values corresponding to the desired properties of the controlled system, e.g. we "place the poles" so that the controlled system has eigenvalues corresponding to a stable stationary state, which is unstable in the autonomous system. Once the eigenvalues

have been chosen, the $l$-coefficients are given by eq. (5.9) and eq. (5.11) can be solved to find the $q, r$-coefficients that determine the control perturbations. To clarify the theory, we proceed with an example.

*Example* For demonstration of the use of linear control theory, we perform a simulation on the computer. As our dynamical system we choose the Hopf normal form fitted to results from experiments on the BZ reaction taken from [12], but altered slightly to fit the normalization introduced in chapter 4 instead of the normalization used in [27]. Thus, the state of the dynamical system is given by

$$\mathbf{x}(t) = 2a(t)(\mathbf{u}\cos\varphi(t) - \mathbf{v}\sin\varphi(t)) \tag{E1}$$

where $a$ and $\varphi$ are given specifically by

$$a(t) = \frac{a_s}{\sqrt{1 + (a_s^2/a_0^2 - 1)e^{-2g'a_s^2 t}}} \tag{E2}$$

and

$$\varphi(t) = \varphi_0 + (\omega_{ss} - g''a_s^2)t - \frac{g''}{2g'}\log\left[1 + \left(\frac{a_o^2}{a_s^2} - 1\right)(1 - e^{-2g'a_s^2 t})\right] \tag{E3}$$

The normal form parameters are the same as used in [12] and can be viewed in table 5.1. They do not, of course, depend on the choice of normalization, since they have been determined from an actual experiment. To perform control on this system, first it is necessary to determine the dimension of the system. Although the state vector is 3-dimensional, the system is in fact 2-dimensional in this context, since the motion of the system can be completely characterized by an amplitude and a relative phase, i.e.

| | |
|---|---|
| $a_s$ | $7.9 \times 10^{-7}$ M |
| $g'$ | $9 \times 10^{10}$ M$^{-2}$ s$^{-1}$ |
| $g''$ | $3 \times 10^{10}$ M$^{-2}$ s$^{-1}$ |
| $\omega_{ss}$ | $0.20$ s$^{-1}$ |

**Table 5.1**: Normal form parameters

$$a = \sqrt{(\mathbf{g}\cdot\mathbf{x})^2 + (\mathbf{h}\cdot\mathbf{x})^2} \qquad \varphi = \arg(\mathbf{g}\cdot\mathbf{x}, \mathbf{h}\cdot\mathbf{x}) \tag{E4}$$

These expressions are the same as in [12] and are thus also independent of the normalization of the eigenvectors.

The system (E1) is thus overall the same as the Hopf normal form for the BZ reaction in [12]. It has a stable limit cycle with the amplitude $a_s$ and a period of $\frac{2\pi}{\omega_{ss}}$. The unstable stationary state encircled by the limit cycle is located at the origin.

The goal of the control is to stabilize the unstable stationary state by changing the motion of the system from the limit cycle by performing the

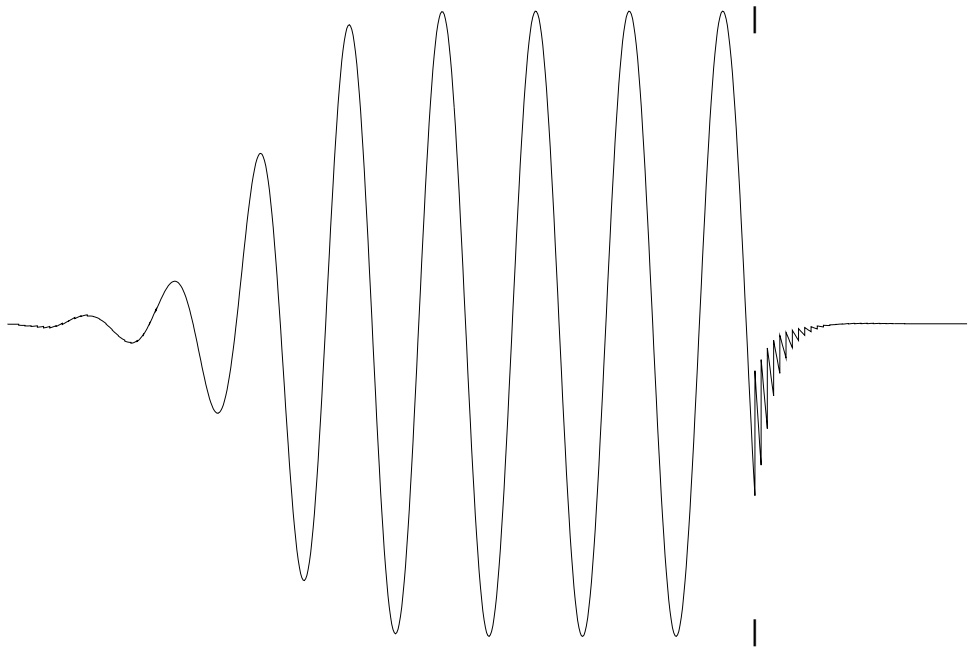

**Figure 5.1**: Control of the Hopf normal form for the BZ reaction. The identification is done at the spiralling out of the system from the unstable stationary state. The control is initiated at the point marked by two vertical lines.

adequate perturbations. The first step in the control algorithm is the identification, and because the identification has to take place close to the state we are supposed to aim for, we start the system close to the unstable stationary state (see fig. 5.1). Immediately we can see from eq. (5.6) that $b_0 = 0$, because the stationary state is located at the origin. The identification is performed with random size perturbations every two seconds of the $Br^-$-concentration, the size varying between $5 \times 10^{-9}$M and $5 \times 10^{-10}$M. From the identification we get the coefficients

$$a_1 = 2.006,\ a_2 = -1.234,\ b_1 = 0.2853,\ b_2 = 0.6720$$

In experimental systems it might be difficult, though, to start the system close to the stationary state, but if the system's quenching parameters have been determined previously, the solution could be to perform a quenching first and then do the identification.

The system is then allowed to spiral out to the limit cycle. To proceed,

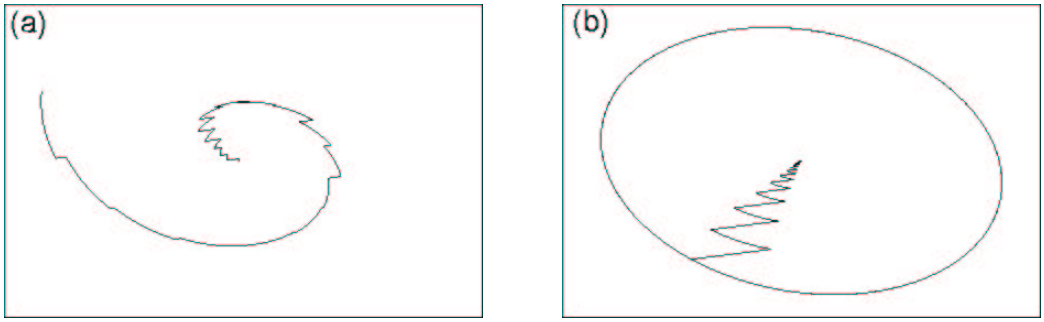


**Figure 5.2**: Phaseplots of (a) the identification, and (b) the control of the Hopf normal form for the BZ reaction.

we choose the eigenvalues of the controlled system to be

$$\rho_1^* = 0.25,\ \rho_2^* = 0.2,\ \rho_3^* = 0.1 - i\,0.2,\ \rho_4^* = 0.1 + i\,0.2$$

i.e. well within the stable area. From eq. (5.9) we know the $l$-coefficients to be

$$\begin{aligned} l_1 &= \rho_1^* + \rho_2^* + \rho_3^* + \rho_4^* \\ l_2 &= -(\rho_1^*\rho_2^* + \rho_1^*\rho_3^* + \rho_1^*\rho_4^* + \rho_2^*\rho_3^* + \rho_2^*\rho_4^* + \rho_3^*\rho_4^*) \\ l_3 &= \rho_1^*\rho_2^*\rho_3^* + \rho_1^*\rho_2^*\rho_4^* + \rho_1^*\rho_3^*\rho_4^* + \rho_2^*\rho_3^*\rho_4^* \\ l_4 &= -\rho_1^*\rho_2^*\rho_3^*\rho_4^* \end{aligned}$$

To get the control coefficients we insert into eq. (5.11) to obtain

$$q_1 = 0.2420,\ q_2 = 3.720 \times 10^{-3},\ r_1 = -0.1038$$

These coefficients are then used to calculate the $k$'th perturbation according to the expression (5.10). The start of the control perturbations are marked by two vertical lines in fig. 5.1. To get another perspective, it can be useful to consider the phaseplots of the system in fig. 5.2. In (a) is shown the phaseplot of the identification, and in (b) is shown the control of the system from the limit cycle to the stationary state. In both figures it is obvious that the control works, but it is critically dependent on getting the right identification. Trying to start the identification on the limit cycle will be unsuccessful. Less critical is the choice of eigenvalues for the pole placement. They only have to be stable and not too close to a numerical value of one.

## 5.2 Nonlinear Control

We shall briefly discuss the concept of nonlinear control theory as described by Petrov and Showalter [22, 23]. At first glance the idea is very similar to

the linear autoregressive control, but there are subtle differences.

There are still two parts, identification and control, but here the two parts are fitted to the same expression. The expression comes from the concept of invariant surfaces for dynamical systems. Using time-delayed and time-forwarded coordinates in phase-space, and assuming that perturbations are performed as perturbations on a bifurcation parameter, the perturbation with index $k+1$ obeys

$$\begin{aligned} w_{k+1} &= L_S(y_k, y_{k-1}, \ldots, y_{k-n}; w_k, w_{k-1}, \ldots, w_{k-n+2}; \\ &\quad (y_{k+n+1} - y_{k+n}), \ldots, (y_{k+2n} - y_{k+2n-1}); \\ &\quad w_{k+n+1}, \ldots, w_{k+2n}) \end{aligned} \tag{5.13}$$

where $L_S$ is a linear function. If the perturbations are too large for a linear description, the more general expression

$$\begin{aligned} w_{k+1} &= S(y_k, y_{k-1}, \ldots, y_{k-n}; w_k, w_{k-1}, \ldots, w_{k-n+2}; \\ &\quad (y_{k+n+1} - y_{k+n}), \ldots, (y_{k+2n} - y_{k+2n-1}); \\ &\quad w_{k+n+1}, \ldots, w_{k+2n}) \end{aligned} \tag{5.14}$$

should be used. $S$ is a nonlinear function of the $4n$ variables.

The idea is then that either (5.13) or (5.14) is used for first identifying the system with random perturbations and subsequently directing the system to the proper state by choosing the time-forwarded coordinates correctly, e.g. trying to stabilize an unstable stationary state can be accomplished by choosing

$$y_{k+n+1} - y_{k+n} = \cdots = y_{k+2n} - y_{k+2n-1} = w_{k+n+1} = \cdots = w_{k+2n} = 0$$

and inserting into the equation for the invariant surface ((5.13) or (5.14)), because the system will obey the equation no matter which values are chosen for the time-forwarded coordinates.

This method does seem more appealing than the method described in section 5.1 using the same equation for both identification and control. It also seems more correct to obtain the control by choosing the value of the desired state itself rather than choosing the eigenvalues. An additional advantage is the straightforward extension to nonlinear cases.

# 6
# Kinetic Spectrometry

Kinetic Spectrometry is the method for finding the Jacobian matrix of a chemical dynamical system. We shall see how perturbations with each of the system's dynamical species will produce identification coefficients that can be combined to yield the exponential of the Jacobian matrix and thus the Jacobian itself. We shall also see, what happens if the system has dynamical modes that are very fast, i.e. if some of the eigenvalues of the Jacobian matrix are so large that motion on the associated manifolds is too fast to be observed by the method. Finally we shall see what results the method provides, experimentally, for the Ce-catalyzed BZ reaction.

## 6.1 Finding the Jacobian Matrix of a Dynamical System

Kinetic Spectrometry uses the same identification process used in control theory. So basically it is just a matter of perturbing the system randomly and reading the output of one of the system's physical properties. This will have to be repeated with all of the dynamical species, though. The only problem is, that it can be difficult to know exactly when the identification has been performed well enough to give the correct results, at least in experimental systems. It is thus important to choose the state of the system with some care to get correct identification, although the method in principle works for all states. On the computer it is easy to insert the system parameters into the model and obtain the Jacobian matrix for direct comparison with the Jacobian matrix calculated from Kinetic Spectrometry. The advantage of the method is that it is not necessary to know the connection between the concentration of the dynamical species and the measured property, even

though the Jacobian matrix depends on the stationary concentrations of the dynamical species.

### 6.1.1 Multiple Identification

Kinetic Spectrometry uses exactly the same method for identifying the system as the one described in chapter 5. To recapitulate, the $n$-dimensional, discrete system equation including perturbations at equidistant $t_k$'s is

$$\mathbf{u}_k = \mathbf{F} \cdot \mathbf{u}_{k-1} + \mathbf{F} \cdot \mathbf{g} w_{k-1} \tag{6.1}$$

Equation (6.1) can then be transformed to the canonical form by a similarity transformation:

$$\mathbf{v}_k = \mathbf{L} \cdot \mathbf{v}_{k-1} + \mathbf{d} w_{k-1} \tag{6.2}$$

with

$$\begin{aligned} \mathbf{v} &= \mathbf{A} \cdot \mathbf{u} \\ \mathbf{L} &= \mathbf{A} \cdot \mathbf{F} \cdot \mathbf{A^{-1}} = \begin{pmatrix} 0 & 1 & 0 & \cdots & 0 \\ 0 & 0 & 1 & \cdots & 0 \\ \vdots & \vdots & \vdots & \ddots & \vdots \\ 0 & 0 & 0 & \cdots & 1 \\ L_{n1} & L_{n2} & L_{n3} & \cdots & L_{nn} \end{pmatrix} \\ \mathbf{d} &= \mathbf{A} \cdot \mathbf{F} \cdot \mathbf{g} \end{aligned} \tag{6.3}$$

The connection with an autoregression equation,

$$\begin{aligned} y_k &= a_1 y_{k-1} + a_2 y_{k-2} + \ldots + a_n y_{k-n} + b_0 + \\ &\quad b_1 w_{k-1} + b_2 w_{k-2} + \ldots + b_n w_{k-n} \end{aligned} \tag{6.4}$$

with $y = \mathbf{h^T} \cdot \mathbf{c}$, $\mathbf{h}$ being the "observation" vector determined from experimental circumstances, was

$$L_{n1} = a_n, L_{n2} = a_{n-1}, \ldots, L_{nn} = a_1$$

Furthermore, which was not shown in chapter 5, it can be shown [13] that

$$\mathbf{d} = \mathbf{C^{-1}} \cdot \mathbf{b} \tag{6.5}$$

where

$$\mathbf{C} = \begin{pmatrix} 1 & 0 & \cdots & & 0 \\ -a_1 & 1 & 0 & & \vdots \\ -a_2 & -a_1 & 1 & \ddots & \\ \vdots & \vdots & \ddots & \ddots & 0 \\ -a_{n-1} & -a_{n-2} & \cdots & -a_1 & 1 \end{pmatrix} \quad \text{and} \quad \mathbf{b} = \begin{pmatrix} b_1 \\ b_2 \\ \vdots \\ b_n \end{pmatrix}$$

Obviously, from the relations (6.3) and (6.5), $\mathbf{A}\cdot\mathbf{F}\cdot\mathbf{g}=\mathbf{C^{-1}}\cdot\mathbf{b}$ and by performing perturbation experiments with $n$ dynamical species, i.e with $n$ linearly independent $\mathbf{g}$'s, this can, due to linearity, be extended to the corresponding matrix equation:

$$\mathbf{A}\cdot\mathbf{F}\cdot\mathbf{G}=\mathbf{C^{-1}}\cdot\mathbf{B} \tag{6.6}$$

with $\mathbf{G}=(\mathbf{g}_1,\ldots,\mathbf{g}_n)$ and $\mathbf{B}=(\mathbf{b}_1,\ldots,\mathbf{b}_n)$. Combining $\mathbf{L}\cdot\mathbf{A}=\mathbf{A}\cdot\mathbf{F}$ with eq. (6.6), we get for invertible $\mathbf{B}$'s:

$$\mathbf{F}=\mathbf{A^{-1}}\cdot\mathbf{L}\cdot\mathbf{A}=\overbrace{\mathbf{G}\cdot\mathbf{B^{-1}}\cdot\mathbf{C}\cdot\mathbf{L}}^{\mathbf{A^{-1}}}\cdot\mathbf{C^{-1}}\cdot\mathbf{B}\cdot\mathbf{G^{-1}} \tag{6.7}$$

By performing at least $3n+1$ measurements of $y_k$ for each of the $n$ linearly independent experiments to get $2n+1$ equations, it is possible to determine the coefficients $a_i$ and $b_i$, and thus *it is possible to find the Jacobian matrix,* $\mathbf{J}$*, including its left and right eigenvectors*, since $\mathbf{F}=e^{\mathbf{J}\Delta t}$.

As we saw in chapter 5, a larger number of measurements is necessary for practical purposes, because all in real chemical systems there will inevitably be some noise. Using SVD on the $y,w$-matrix will produce the correct coefficients.

Because the matrices, $\mathbf{C}$ and $\mathbf{L}$ can be chosen from any of the $n$ independent experiments, we would expect the $a$-coefficients to be the same in each experiment. The $b$-coefficients, however, must be different for each experiment.

### 6.1.2 Conditions

There are, of course, certain conditions that must apply, before we can expect any success with the method. There is the matter of choosing the perturbations carefully, which was described in chapter 5.

The "observation vector", $\mathbf{h}$, must also be chosen to fulfil a condition, *the observability condition*. The observability condition tells us whether observing the $y$'s will allow us to determine the $\mathbf{c}$'s of the unperturbed system. It can be shown [13] that this is the case, if the matrix

$$\mathbf{A}=\begin{pmatrix}\mathbf{h^T}\\ \mathbf{h^T}\cdot\mathbf{F}\\ \mathbf{h^T}\cdot\mathbf{F^2}\\ \vdots\\ \mathbf{h^T}\cdot\mathbf{F^{n-1}}\end{pmatrix}$$

has rank $n$.

The perturbation vectors, $\mathbf{g}_i$, must fulfil *the controllability condition*. The controllability condition expresses, whether the $\mathbf{g}$'s will excite all $n$ modes of the system. This is the case, if the matrix

$$(\mathbf{g}, \mathbf{F} \cdot \mathbf{g}, \mathbf{F^2} \cdot \mathbf{g}, \ldots, \mathbf{F^{n-1}} \cdot \mathbf{g})$$

also has rank $n$ [13].

Finally, $\Delta t$ must be chosen correctly, because $\mathbf{F}$ depends on $\Delta t$. Thus, choosing $\Delta t$ can determine, whether the system meets the observability and controllability conditions. Experimentally, because $\mathbf{F}$ is the aim of the experiment, $\Delta t$ must be chosen by trial and error. This issue will be addressed in more detail in section 6.2.1.

### 6.1.3 Using the Method on Oscillating Systems

In order to avoid nonlinear effects as much as possible it is more convenient to work with a chemical system that has a stable stationary point, e.g. on the stable side of a supercritical Hopf bifurcation. This will make the identification much easier. The chemistry on the stable side does not differ much from the chemistry on the unstable side, and the eigendirections do not differ much either, only the stability of two of them differs.

In experimental applications it is worth remembering that the matrices $\mathbf{L}$ and $\mathbf{F}$ have the same eigenvalues. This is practical for assessing whether one is choosing $\Delta t$ correctly, since it only requires one series of perturbations to determine $\mathbf{L}$. For a system close to a Hopf bifurcation one would expect to find two of the eigenvalues of $\mathbf{L}$ as a complex pair with numerically small real parts and imaginary parts corresponding to the period of the damped oscillations. Measuring the period is easily done by applying a single, large perturbation to the system and observing the response.

Thus, choosing the parameters of the system to be close to a supercritical Hopf bifurcation will be an advantage, although the method in principle works for all parameter values.

### 6.1.4 Kinetic Spectrometry on the Oregonator

To demonstrate the use of Kinetic Spectrometry, we shall apply the method to the Oregonator and compare the result with the Jacobian Matrix calculated directly from eq. (3.8). The rate constants are taken from [2], and they are listed together with the chosen parameters in table 6.1. With these values, the system has a stable stationary state, $\mathbf{c}_s = (\mathrm{X}_s,\ \mathrm{Y}_s,\ \mathrm{Z}_s)$

| | |
|---|---|
| $k_1$ | 2.0 $s^{-1}$ $M^{-2}$ |
| $k_2$ | 3.0 $\times 10^6$ $s^{-1}$ $M^{-2}$ |
| $k_3$ | 42 $s^{-1}$ $M^{-2}$ |
| $k_4$ | 3.0 $\times 10^3$ $s^{-1}$ $M^{-2}$ |
| $k_5$ | 0.167 $s^{-1}$ $M^{-1}$ |
| $f$ | 0.79 |
| A | 0.01097 M |
| $j$ | 3.0 $\times 10^{-5}$ $s^{-1}$ |

**Table 6.1**: Reaction rate constants and parameter values used in the application of Kinetic Spectrometry on the Oregonator.

= (3.230, 19.70, 17.72) $\times$ $10^{-8}$ M. It was found that a $\Delta t$ of 2.5 s delivered satisfactory results. The perturbation magnitude, $w_k$, was chosen to be 2.5 $\times 10^{-11}$ M at $t_k$'s with $\frac{t_k}{\Delta t}$ multipla of 7, 13 or 17. The coefficients were calculated on the basis of 1500 measurements of the $Ce^{4+}$-concentration. A part of the time series can be seen in fig. 6.1. The coefficients calculated from the time series in fig. 6.1 are

$$\begin{aligned}(a_1, a_2, a_3) &= (2.274, -1.666, 0.3506) \quad b_0 = 7.339 \times 10^{-9}\text{M} \\ (b_1, b_2, b_3) &= (0.6419, -1.121, 0.3505)\end{aligned}$$

The remaining two time series with additions of $HBrO_2$ and $Br^-$ respectively provided the same $a$-coefficients and the $\mathbf{b}$-vectors

$$\mathbf{b}_{HBrO_2} = \begin{pmatrix} 1.640 \\ -1.230 \\ 8.441 \times 10^{-4} \end{pmatrix} \qquad \text{and} \qquad \mathbf{b}_{Br^-} = \begin{pmatrix} -0.1543 \\ -0.1099 \\ 1.374 \times 10^{-4} \end{pmatrix}$$

We can now form the matrices $\mathbf{L}, \mathbf{C}, \mathbf{B}$ and $\mathbf{G}$ ($\mathbf{G}$ is equal to the 3D identity matrix), and insert into eq. (6.7). Taking the logarithm of $\mathbf{F}$ and dividing by $\Delta t$ provides us with the Jacobian matrix (in units of $s^{-1}$)

$$\mathbf{J} = \begin{pmatrix} -0.1332 & -0.0750 & 0.0000 \\ -0.5904 & -0.1190 & 0.1320 \\ 0.9156 & 0.0002 & -0.1671 \end{pmatrix}$$

This should be compared with the Jacobian matrix calculated directly from the model

$$\mathbf{J} = \begin{pmatrix} -0.1332 & -0.0751 & 0 \\ -0.5909 & -0.1188 & 0.132 \\ 0.9162 & 0 & -0.1670 \end{pmatrix}$$

The agreement between the two matrices is excellent, and Kinetic Spectrometry obviously works in this case.

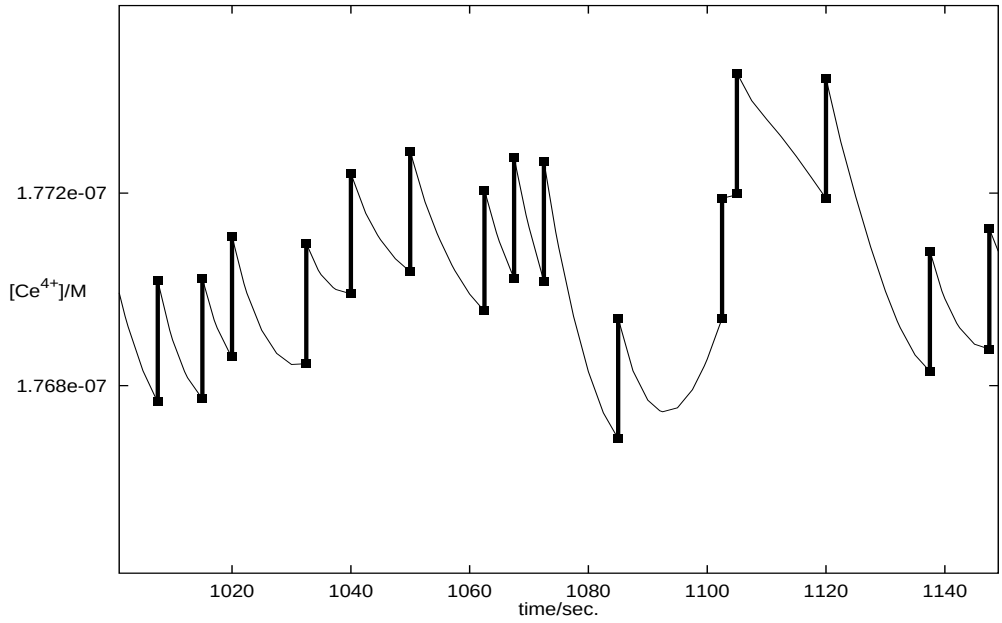


**Figure 6.1**: Part of the time series of the identification of the Oregonator. The vertical, bold lines correspond to additions of $Ce^{4+}$. The corresponding phaseplot can be seen on the front page, where the stationary state is marked by a ■.

It should be mentioned, though, that the agreement between the two matrices is still good, when applying larger perturbations, but not as good as the example shown here. This is due to the larger inaccuracies arising when describing the nonlinear system state with a linear approximation. The larger the perturbations, the larger the deviations from the linear description. See also section 6.3.2.

Although choosing $\Delta t$ in principle can be done by inspection of the model, it has been done by trial and error in this case. However, it is not surprising to find $\Delta t = 2.5$ s, knowing that the eigenvalue of the Jacobian matrix with the numerically largest real part is -0.41, and thus that the characteristic time, $\tau$, of the system is equal to $\frac{1}{0.41}$ s $\approx 2.5$ s.

## 6.2 Kinetic Spectrometry with a Reduced Number of Dimensions

In some settings (e.g. experimental situations) it might not be possible or desirable to sample fast enough to get information about all the dynamical modes of the system. Thus, it could be necessary to know exactly what

can actually be determined, when one works with a reduced number of dimensions. We shall discover both the consequences on the determination of the system's properties when retaining a description of the system with the full dimension and when trying to determine the Jacobian matrix with the reduced number of dimensions as if it was the full number of dimensions.

### 6.2.1 Slow and Fast Modes

First of all it is necessary to make clear that a dynamical mode is a slang term for motion on the manifolds that the eigenvectors of the Jacobian matrix are tangent to, i.e. a slow mode corresponds to a manifold on which the motion towards the stable stationary point (or away from the unstable stationary point) is slow.

Consider a chemical system close to a supercritical Hopf bifurcation with $n$ dynamical modes, $p$ slow modes and $q$ fast modes, i.e. $n = p + q$. In real chemical systems close to a supercritical Hopf bifurcation all real eigenvalues are negative, which means that the exponential of the eigenvalues are less than one. When one speaks of slow and fast modes it is of course a relative matter, both between the individual modes, and in comparison with the sampling interval, $\Delta t$. The definition of a fast mode in this context is a mode, whose eigenvalue is large enough numerically for all motion on the manifold associated with this eigenvalue to have ceased after one sampling interval. To express it mathematically, it means that $|\rho_i| \gg |\rho_j| \ll 1$ for $i = 1, \ldots, p$ and $j = p + 1, \ldots, n$, where $\rho$ are eigenvalues of $\mathbf{F}$.

Thus choosing a sampling interval must be a compromise between sampling fast enough to get all information about the slow modes, and slow enough in order to maintain the fast modes as fast modes, i.e. to get a clear separation of the slow and the fast modes.

### 6.2.2 Reduction in Eigenvector-Space

The dynamics of the $n$-dimensional system in concentration-space is described in the linear approximation by equation (6.1). We assume that the right eigenvectors of $\mathbf{F}$, $\mathbf{e}_1, \ldots, \mathbf{e}_n$, exist, and that there are no degeneracies between them. We can then perform a similarity transformation with the matrix $\mathbf{U} = (\mathbf{e}_1 \ldots \mathbf{e}_n)$ to transform equation (6.1) from concentration-space to eigenvector-space:

$$\begin{aligned} \mathbf{x}_k &= \underbrace{\mathbf{U}^{-1} \cdot \mathbf{F} \cdot \mathbf{U}}_{\mathbf{R}_n} \cdot \mathbf{x}_{k-1} + \underbrace{\mathbf{U}^{-1} \cdot \mathbf{F} \cdot \mathbf{U}}_{\mathbf{R}_n} \cdot \mathbf{U}^{-1} \cdot \mathbf{g} w_{k-1} \qquad (6.8) \\ \mathbf{x} &= \mathbf{U}^{-1} \cdot \mathbf{u} \end{aligned}$$

Since $\mathbf{R}_n$ is a diagonal matrix with the eigenvalues of $\mathbf{F}$ in the diagonal, equation (6.8) describes the linear dynamics of the system in eigenvector-space. With the system coordinates along the eigenvectors it is relatively easy to find the projection along the $p$ slow modes. First we need to form the projection operators $\mathbf{\Pi}$ and $\hat{\mathbf{\Pi}}$:

$$\hat{\mathbf{\Pi}} = \begin{pmatrix} \mathrm{I}_p \\ \dots \\ 0_{q\times p} \end{pmatrix} \qquad \mathbf{\Pi} = \begin{pmatrix} \mathrm{I}_p \vdots 0_{p\times q} \end{pmatrix}$$

$\mathbf{I}_p$ is the $p \times p$ identity matrix. Some of the properties of $\mathbf{\Pi}$ and $\hat{\mathbf{\Pi}}$ are evidently:

$$\mathbf{P} = \hat{\mathbf{\Pi}} \cdot \mathbf{\Pi} = \left(\begin{array}{c|c} \mathrm{I}_p & 0 \\ \hline 0 & 0 \end{array}\right) \qquad \text{and} \qquad \mathbf{\Pi} \cdot \hat{\mathbf{\Pi}} = \mathbf{I}_p$$

We now assume that $\Delta t$ is chosen so that $|\rho_j| \ll 1$ for $j = p+1, \dots, n$, i.e. $\mathbf{R}_n \cdot \mathbf{P} \approx \mathbf{R}_n$ to a very good approximation. Thus equation (6.8) can be manipulated in the following way[1]:

$$\begin{aligned} \mathbf{x}_k &= \mathbf{R}_n \cdot \mathbf{P} \cdot \mathbf{x}_{k-1} + \mathbf{R}_n \cdot \mathbf{P} \cdot \mathbf{U}^{-1} \cdot \mathbf{g} w_{k-1} \\ \mathbf{\Pi} \cdot \mathbf{x}_k &= \underbrace{\mathbf{\Pi} \cdot \mathbf{R}_n \cdot \hat{\mathbf{\Pi}}}_{\mathbf{R}_p} \cdot \mathbf{\Pi} \cdot \mathbf{x}_{k-1} + \underbrace{\mathbf{\Pi} \cdot \mathbf{R}_n \cdot \hat{\mathbf{\Pi}}}_{\mathbf{R}_p} \cdot \mathbf{\Pi} \cdot \mathbf{U}^{-1} \cdot \mathbf{g} w_{k-1} \\ \mathbf{x'}_k &= \mathbf{R}_p \cdot \mathbf{x'}_{k-1} + \underbrace{\mathbf{R}_p \cdot \mathbf{\Pi} \cdot \mathbf{U}^{-1} \cdot \mathbf{g}}_{\tilde{\mathbf{d}}'} w_{k-1} \end{aligned} \tag{6.9}$$

Equation (6.9) is the $p$-dimensional equivalent of equation (6.8), but it only applies to the chemical system as long as the $p$ dimensions include *all* the slow modes of the system. If that criteria is fulfilled, it is evident that using the method and treating the system as $p$-dimensional produces the correct eigenvalues for the system, but only the slow ones. Equation (6.9) can be transformed further to the canonical form in $p$ dimensions:

$$\mathbf{v'}_k = \mathbf{L}' \cdot \mathbf{v'}_{k-1} + \mathbf{d}' w_{k-1} \tag{6.10}$$

$$\mathbf{v}' = \mathbf{A}' \cdot \mathbf{x}' \qquad \mathbf{L}' = \mathbf{A}' \cdot \mathbf{R}_p \cdot \mathbf{A'}^{-1}$$

[1] Primed objects are $p$-dimensional

As with the transformation from eq. (6.1) to eq. (6.8) where the columns of $\mathbf{U}$ were the right eigenvectors of $\mathbf{F}$, the columns of $\mathbf{A}'$ must be the right eigenvectors of $\mathbf{L}'$. Assuming that $\mathbf{L}'$ does not have any multiple eigenvalues, $\mathbf{A}'$ can be written as [35]:

$$\mathbf{A}' = \begin{pmatrix} 1 & 1 & \cdots & 1 \\ \rho_1 & \rho_2 & \cdots & \rho_p \\ \rho_1^2 & \rho_2^2 & \cdots & \rho_p^2 \\ \vdots & \vdots & & \vdots \\ \rho_1^{p-1} & \rho_2^{p-1} & \cdots & \rho_p^{p-1} \end{pmatrix}$$

As in $n$ dimensions it also applies in $p$ dimensions, that

$$\mathbf{A}' \cdot \tilde{\mathbf{d}}' \;=\; \mathbf{d}' \;=\; {\mathbf{C}'}^{-1} \cdot \mathbf{b}' \tag{6.11}$$

Equations (6.11) and (6.9) apply for perturbations with all $n$ chemical species, and due to linearity they lead to the corresponding matrix equation:

$$\tilde{\mathbf{D}}' = \mathbf{R}_p \cdot \mathbf{\Pi} \cdot \mathbf{U}^{-1} \cdot \mathbf{G} = {\mathbf{A}'}^{-1} \cdot {\mathbf{C}'}^{-1} \cdot \mathbf{B}'$$

where $\tilde{\mathbf{D}}'$ and $\mathbf{B}'$ are $p \times n$ matrices and $\mathbf{G}$ is an $n \times n$ matrix. This equation can be rearranged to:

$$\mathbf{\Pi} \cdot \mathbf{U}^{-1} = \mathbf{R}_p^{-1} \cdot {\mathbf{A}'}^{-1} \cdot {\mathbf{C}'}^{-1} \cdot \mathbf{B}' \cdot \mathbf{G}^{-1}$$

Writing it explicitly, with the rows of $\mathbf{U}^{-1}$ as the left eigenvectors of $\mathbf{F}$, defined by the normalization, $\mathbf{e}^i \cdot \mathbf{e}_j = \delta_{ij}$, it gets the appearance:

$$\begin{pmatrix} \mathbf{e}^1 \\ \vdots \\ \mathbf{e}^p \end{pmatrix} = \mathbf{R}_p^{-1} \cdot {\mathbf{A}'}^{-1} \cdot {\mathbf{C}'}^{-1} \cdot \mathbf{B}' \cdot \mathbf{G}^{-1} \tag{6.12}$$

All the terms on the righthandside of eq. (6.12) can be determined from experiments. The eigenvalues of $\mathbf{L}$ are determined from the $a$-coefficients and can be inserted into $\mathbf{R}_p$ and $\mathbf{A}'$. The $a$-coefficients can be inserted directly into $\mathbf{C}'$, and the $b$-coefficients from $n$ different experiments can be inserted into $\mathbf{B}'$. The conditions of these experiments will also automatically provide the $\mathbf{G}$ matrix. Since $\mathbf{F}$ has the same eigenvectors as the Jacobian, $\mathbf{J}$, the result in equation (6.12) means that *the* p *slow* n*-dimensional left eigenvectors of the Jacobian matrix can be determined by perturbing with* n *independent species*. Compared with quenching theory this is an improvement, because here it is possible to determine *all* the slow left eigenvectors of the Jacobian,

whereas in quenching theory it was only possible to determine the left eigenvectors corresponding to the oscillating modes as long as only one species (or one combination of species) can be observed.

The problem with this result in experimental settings is of course that $n$ usually is unknown, and it can be difficult to determine. Even in the BZ reaction, the number of dynamical species is not known with absolute certainty.

*Example* To test the validity of eq. (6.12) the linear system

$$\dot{\mathbf{u}} = \mathbf{J} \cdot \mathbf{u}$$

was chosen with $\mathbf{J}$ equal to

$$\mathbf{J} = \begin{pmatrix} -0.1 & 0 & 0.2 & 0 \\ 0 & -0.1 & 0.3 & 0.2 \\ 0.2 & -0.3 & -0.1 & 0 \\ 0 & 0.1 & 0 & -3 \end{pmatrix}$$

$\Delta t$ was chosen equal to 5, which determined the eigenvalues of $\mathbf{F} = e^{\mathbf{J}\Delta t}$ to be equal to $\{0.3321 \pm i\ 0.6819,\ 0.4987,\ 2.379 \times 10^{-7}\}$. Clearly, in this case, $p = 3$. Kinetic Spectrometry was then performed on the system with the dimension in the identification equal to 3, and the perturbations were performed as additions to the four different coordinates of the system to simulate a chemical system.

Having done that, the eigenvectors were then calculated according to eq. (6.12), which gave the result

$$\begin{pmatrix} \mathbf{l} \\ \mathbf{m} \\ \mathbf{e}^3 \end{pmatrix} = \begin{pmatrix} 0.1579 & -0.1021 & 0.4692 & -0.009266 \\ -0.3882 & 0.6217 & 0.08963 & 0.1063 \\ -0.3158 & 0.2025 & 0.06180 & 0.03539 \end{pmatrix}$$

remembering that $\mathbf{e}^1 = \bar{\mathbf{e}}^2 = \mathbf{l} + i\mathbf{m}$.

This should be compared to the eigenvectors calculated directly from $\mathbf{J}$

$$\begin{pmatrix} \mathbf{l} \\ \mathbf{m} \\ \mathbf{e}^3 \end{pmatrix} = \begin{pmatrix} 0.1579 & -0.1021 & 0.4692 & -0.009267 \\ -0.3882 & 0.6217 & 0.08963 & 0.1063 \\ -0.3158 & 0.2025 & 0.06180 & 0.03539 \end{pmatrix}$$

Again, the similarity is striking with four significant digits, which is probably due to the system being linear and the clear separation of slow and fast modes. Also in these simulations no noise was added to the measurements. Noise effects are treated in section 6.3.2.

### 6.2.3 Reduction in Concentration-Space

Equation (6.9) tells us what eigenvalues to expect, but it does not say much about the $p$-dimensional "Jacobian" that will be determined by applying Kinetic Spectrometry in $p$ dimensions.

The aim of determining a $p$-dimensional Jacobian matrix is to capture the essential dynamics of the system, i.e. the dynamics of the slow modes, in a $p$-dimensional description in concentration-space. The strategy is (starting in concentration-space) to "diagonalize" the fast subspace first, and then project onto a $p$-dimensional concentration-space. This corresponds to the system's response to perturbations, where the initial very fast motion along the fast eigenvectors is finished, before the motion in the slow subspace has proceeded to any appreciable extension.

Consider eq. (6.1). Since we are only looking at the first $p$ coordinates of the system, i.e. a projection of the system onto the first $p$ coordinates in concentration-space, we have $\mathbf{P} \cdot \mathbf{u} = \mathbf{u}$, and $\mathbf{P} \cdot \mathbf{g} = \mathbf{g}$. We want to perform a similarity transformation that preserves the first $p$ coordinates of $\mathbf{u}$, but also preserves the slow subspace. This can be achieved with the matrix

$$\tilde{\mathbf{A}} = \left( \begin{array}{c|ccc} \mathrm{I}_p & & & \\ \hline 0_{q\times p} & \mathbf{e}_{p+1} & \cdots & \mathbf{e}_n \end{array} \right)$$

where $\mathbf{e}_{p+1}, \ldots, \mathbf{e}_n$ are the $q$ fast right eigenvectors of $\mathbf{F}$. One of the properties of $\tilde{\mathbf{A}}$ is that $\mathbf{u} = \tilde{\mathbf{A}}^{-1} \cdot \mathbf{u}$ and $\mathbf{g} = \tilde{\mathbf{A}}^{-1} \cdot \mathbf{g}$. By applying $\tilde{\mathbf{A}}$ to equation (6.1) in the same way as $\mathbf{U}$, we get:

$$\mathbf{u}_k = \tilde{\mathbf{F}} \cdot \mathbf{u}_{k-1} + \tilde{\mathbf{F}} \cdot \mathbf{g} w_{k-1} \tag{6.13}$$

with

$$\tilde{\mathbf{F}} = \tilde{\mathbf{A}}^{-1} \cdot \mathbf{F} \cdot \tilde{\mathbf{A}} = \begin{pmatrix} \tilde{F}_{11} & \ldots & \tilde{F}_{1p} & 0 & \ldots & & 0 \\ \vdots & & \vdots & \vdots & & & \vdots \\ \tilde{F}_{p1} & \ldots & \tilde{F}_{pp} & 0 & \ldots & & 0 \\ \tilde{F}_{p+1,1} & \ldots & \tilde{F}_{p+1,p} & \rho_{p+1} & 0 & \ldots & 0 \\ \vdots & & \vdots & 0 & \rho_{p+2} & \ddots & \vdots \\ & & & \vdots & \ddots & \ddots & 0 \\ \tilde{F}_{n1} & \ldots & \tilde{F}_{np} & 0 & \ldots & 0 & \rho_n \end{pmatrix}$$

Inserting $\mathbf{P}\cdot\mathbf{u}=\mathbf{u}$, and $\mathbf{P}\cdot\mathbf{g}=\mathbf{g}$ into equation (6.13) and multiplying from the left by $\mathbf{\Pi}$ results in:

$$\mathbf{u}'_k = \underbrace{\mathbf{\Pi}\cdot\tilde{\mathbf{F}}\cdot\hat{\mathbf{\Pi}}}_{\mathbf{F}'}\cdot\mathbf{u}'_{k-1} + \underbrace{\mathbf{\Pi}\cdot\tilde{\mathbf{F}}\cdot\hat{\mathbf{\Pi}}}_{\mathbf{F}'}\cdot\mathbf{g}'w_{k-1} \tag{6.14}$$

which is an equation in a $p$-dimensional concentration-space. Thus we can conclude that applying the method in $p$ dimensions will determine $\mathbf{F}'$ as the exponential of the Jacobian times $\Delta t$, i.e. $\mathbf{F}'=e^{\mathbf{J}'\Delta t}$ , as long as the $p$ dimensions include *all* the slow modes. This is evident from the fact that the eigenvalues of $\mathbf{F}'$ are same as the eigenvalues of $\mathbf{R}_p$, i.e. there exists a similarity transformation that transforms eq. (6.14) to eq. (6.9). Consider $\tilde{\mathbf{F}}$, which has the same eigenvalues as $\mathbf{F}$. It is easily seen that the eigenvalues of $\tilde{\mathbf{F}}$ are $\rho_{p+1},\ldots,\rho_n$ together with the eigenvalues of $\mathbf{F}'$, i.e. the remaining $p$ eigenvalues of $\mathbf{F}$, $\rho_1,\ldots,\rho_p$.

The question is then which $p$ species to choose for perturbing the system. A good suggestion would be those species that are able to quench oscillations in the system. There is one condition, though. The species must quench the oscillations by itself, not because it immediately reacts to produce another species that quenches oscillations. Taking the BZ reaction as an example, having determined the system to have 3 slow modes, one should choose $HBrO_2$, $Br^-$, and $Ce^{4+}$ for perturbing the system. The result could then be compared with the Oregonator, which uses precisely those three species for describing the system.

### 6.2.4 Constructing a Model

We want to estimate, whether trying to construct a model on the basis of the $p$-dimensional Jacobian matrix will provide satisfactory results. To give an impression of the relationship between $\mathbf{F}$ and $\mathbf{F}'$, we consider the case where $n=4$ and $p=3$. With $\mathbf{e}_4^{\mathrm{T}}=(e_{41},e_{42},e_{43},e_{44})$ , $\mathbf{F}'$ gets the appearance:

$$\mathbf{F}' = \begin{pmatrix} F_{11}-F_{41}\frac{e_{41}}{e_{44}} & F_{12}-F_{42}\frac{e_{41}}{e_{44}} & F_{13}-F_{43}\frac{e_{41}}{e_{44}} \\ F_{21}-F_{41}\frac{e_{42}}{e_{44}} & F_{22}-F_{42}\frac{e_{42}}{e_{44}} & F_{23}-F_{43}\frac{e_{42}}{e_{44}} \\ F_{31}-F_{41}\frac{e_{43}}{e_{44}} & F_{32}-F_{42}\frac{e_{43}}{e_{44}} & F_{33}-F_{43}\frac{e_{43}}{e_{44}} \end{pmatrix}$$

In general each element of $\mathbf{F}'$ contains terms from all the missing species and all the fast modes. Thus, trying to construct a $p$-dimensional model for an $n$-dimensional system in accordance with the $p$-dimensional Jacobian takes into consideration the $q$ dimensions that are left out. This is accomplished

automatically by applying the method, since each element in the Jacobian contains the appropriate number of correctional terms. To get a realistic model then only requires that the $p$ dimensions include all the slow modes in order to get $\mathbf{F}'$ right.

To get another perspective, consider the case where the $n$-dimensional system has been found to have a supercritical Hopf bifurcation at a certain parameter value. One would think that if Kinetic Spectrometry was applied to the system in $p$ dimensions, the $p$-dimensional system based on the $p$-dimensional Jacobian matrix would have a supercritical Hopf bifurcation at the same parameter value and thus the same qualitative behaviour.

*Example* To illustrate the importance of not excluding any slow modes we consider two examples with $n = 4$ and $p = 3$. The first simulation was performed on the same model as in the example in section 6.2.2, i.e. $\mathbf{F}$ has the eigenvalues $\{0.3321 \pm i\ 0.6819,\ 0.4987,\ 2.379 \times 10^{-7}\}$. The results were (with $\tilde{\mathbf{J}}$ as the predicted result, and $\mathbf{J}'$ as the result from the sampling):

$$\tilde{\mathbf{J}} = \begin{pmatrix} -0.1 & -0.0003485 & 0.2 \\ 0 & -0.04968 & 0.3 \\ 0.2 & -0.2949 & -0.1 \end{pmatrix}$$

$$\mathbf{J}' = \begin{pmatrix} -0.1000 & -0.0003268 & 0.2000 \\ -0.0000 & -0.04964 & 0.3000 \\ 0.2000 & -0.2949 & -0.09998 \end{pmatrix}$$

The second simulation was also performed on a linear system. With $\Delta t$ equal to 5 as in the first case, and the eigenvalues of $\mathbf{F}$ being equal to $\{0.5096 \pm i\ 0.7087,\ 0.2929,\ 0.2231\}$, the results were:

$$\tilde{\mathbf{J}} = \begin{pmatrix} -0.1 & -0.1 & 0.2 \\ 0 & -0.1 & 0.3 \\ 0.2 & -0.2 & -0.1 \end{pmatrix}$$

$$\mathbf{J}' = \begin{pmatrix} -0.05724 & -0.06336 & 0.2318 \\ 0.01905 & -0.04229 & 0.3228 \\ 0.1844 & -0.2197 & -0.1611 \end{pmatrix}$$

In the second case the mode corresponding to the eigenvalue 0.2231 was left out.

The difference in the last case, where no mode is fast compared with the others, is quite big considering that the simulation has been performed on a linear model, where the method otherwise works perfectly. In the first case, where the mode corresponding to the eigenvalue $2.379 \times 10^{-7}$ is fast

in comparison with the others, the difference is hardly visible. It should be mentioned that the result is equally good when leaving out any of the four coordinates.

### 6.2.5 How to Determine the Number of Slow Modes

The question that has to be answered when using Kinetic Spectrometry experimentally is: "What is the number of slow modes"? Equally, one could ask how many dimensions in the autoregression equation (6.4) should be used? One method is the one used in [21], where they plot the error between the actual reading, $y_k$, and the one calculated from the autoregression equation as a function of the dimension. This may not work, though, in actual experiments due to experimental noise, which would be the dominating error.

A heuristic approach to the matter is to calculate the $a$ and $b$-coefficients with different dimensions and then calculate the eigenvalues on that basis. This should then be compared to the behaviour of the Oregonator in the same situation.

*Example* To get a grip on this approach, we have a look at the Oregonator when trying to calculate its eigenvalues in two, three, and four dimensions. For this purpose we use the time series shown in figure 6.1 with additions of $Ce^{4+}$ to the system, i.e. the same time series used in the example in section 6.1.4. This time series was used to determine the $a$-coefficients, which were then inserted into the $\mathbf{L}$ matrix. The eigenvalues in two, three, and four dimensions respectively were calculated to be

$$\begin{aligned}(\rho_1, \rho_2) &= (0.9514 + i0.2356, 0.9514 - i0.2356)\\ (\rho_1, \rho_2, \rho_3) &= (0.9582 + i0.2504, 0.9582 - i0.2504, 0.3574)\\ (\rho_1, \rho_2, \rho_3, \rho_4) &= (0.9582 + i0.2504, 0.9582 - i0.2504, 0.3550, -0.6526)\end{aligned}$$

Knowing that the real dimension is three, we can understand the result in two dimensions. It is almost correct for the two complex eigenvalues, but not exactly, because a slow mode was left out. The way to spot three as the correct number of slow modes is that the method provides an impossible eigenvalue in four dimensions, i.e. the eigenvalue -0.6526, because $\mathbf{F}$ can not have negative eigenvalues. Apart from that, the method still provides the remaining three eigenvalues correctly. Thus, we can conclude that the fourth dimension is superfluous. We could expect to see a similar pattern in experiments also.

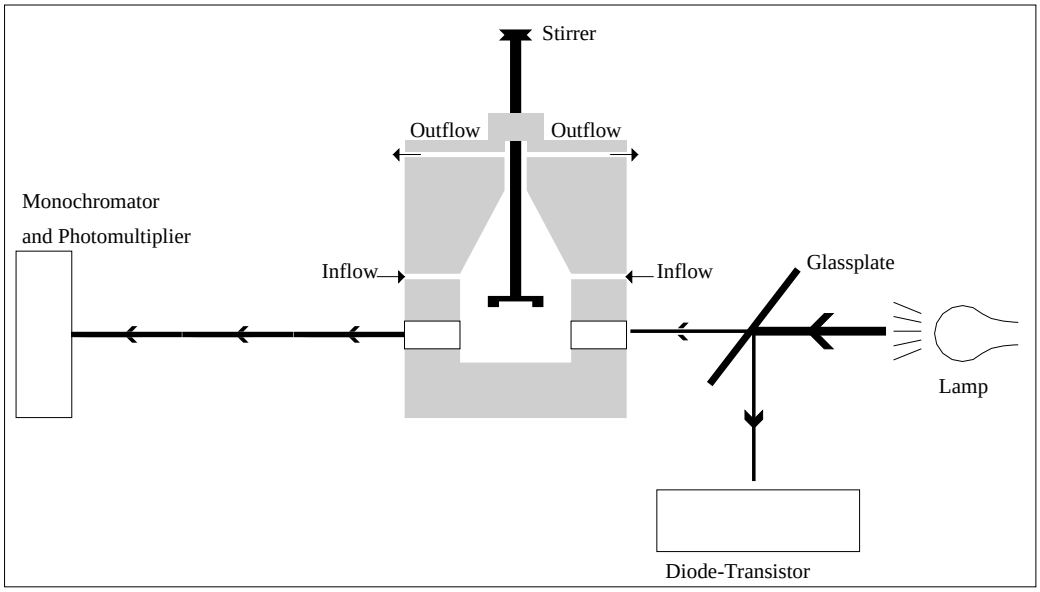


**Figure 6.2**: Schematic presentation of the CSTR.

## 6.3 Experiments

In this section we investigate Kinetic Spectrometry in real experiments on the Ce-catalyzed BZ reaction at conditions similar to the conditions of the quenching experiments by Sørensen and Hynne [27]. Also, we have to examine the response of the method to noise in the simulations to see what influence experimental noise, which is inevitable, has on the determination of the Jacobian matrix.

### 6.3.1 Experimental Setup

The experiments on the Ce-catalyzed BZ reaction were carried out in a CSTR with three different flows. The flows were supplied by two independent burettes for each flow, so that one could be filled from a reservoir while the other was supplying the flow, and vice versa. A full description of this principle can be found in [27]. The principle of the CSTR (see fig. 6.2) is then the following: Fresh reactant species are flown into the cell close to the stirrer. The excess of mixture is removed by suction at the top of the cell, keeping the volume of the reaction mixture constant. Light from an incandescent lamp is shone through the Plexiglas cell, and the absorption wavelength is selected by the monochromator before the light enters the photomultiplier. A semi-transparent quartz glassplate was put into the lightbeam before en-

| Flow species | High flow rate | Low flow rate |
|---|---|---|
| $Ce_2(SO_4)_3$ | 0.00025 M | 0.00025 M |
| Malonic acid | 0.501 M | 0.501 M |
| $KBrO_3$ | 0.024 M | 0.036 M |

**Table 6.2**: Contents of the three flow-solutions. The solvent was 1 M sulfuric acid in each case. The high flow rate was a specific flow rate of 5.08 $\times 10^{-5}$ $s^{-1}$, the low flow rate 2.54 $\times 10^{-5}$ $s^{-1}$.

tering the cell, reflecting part of the light into a diode-transistor to get a reference measurement of the output from the lamp in order to make corrections for any fluctuations in the lamp output. The wavelength selected on the monochromator was 330 nm, because $Ce^{4+}$ has an absorption maximum at 320 nm. 330 nm was selected over 320 nm, because the Plexiglas of the cell gave a resulting maximum at 330 nm.

Just as in [27] these experiments were conducted with three separate flows with equal flow rates. The flow solutions are listed in table 6.2. The materials used for the flows are listed in table 6.3. Equivalently to [27] the temperature was kept constant at 30.0 $\pm$ 0.02°C by maintaining a flow of preheated water in contact with the cell. The fine tuning of the temperature was done with a temperature sensor in the reaction mixture. If the temperature was a little too low, the sensor would send a signal to the voltage control of an exterior lamp which would then shine on the cell, until the temperature was high enough.

As mentioned in chapter 4, Sørensen and Hynne worked close to a supercritical Hopf bifurcation on the unstable side. For the Kinetic Spectrometry experiments it is necessary to work on the stable side of the Hopf bifurcation. This can be done by either lowering the specific flow rate or the bromate concentration. Both options, named the high and low flow rates in table 6.2, were tried. Sørensen and Hynne used a 0.036 M bromate solution in 1 M sulfuric acid at the high flow rate.

### 6.3.2 Noise Effects

From section 6.1.4 we remember that the real Jacobian matrix of the Oregonator model has the appearance

$$\mathbf{J} = \begin{pmatrix} -0.1332 & -0.0751 & 0 \\ -0.5909 & -0.1188 & 0.132 \\ 0.9162 & 0 & -0.1670 \end{pmatrix}$$

with the chosen parameters. When performing Kinetic Spectrometry as in

| Compound | Company | Product number |
|---|---|---|
| $Ce_2(SO_4)_3$ anh. 99.9 % | Heraeus | 001181 |
| $CH_2(COOH)_2$ 99 % | Aldrich | M 129-6 |
| $KBrO_3$ r.g. | Riedel-de Haën | 30205 |
| $H_2SO_4$ 95 - 98 % | Baker | 6027 |

**Table 6.3**: Materials used for the flows in the CSTR.

section 6.1.4 but with the perturbation magnitude, $w_k = 2.5 \times 10^{-9}$, to make it a bit more realistic, the Jacobian matrix from the sampling is

$$\mathbf{J} = \begin{pmatrix} -0.1327 & -0.0740 & -0.0001 \\ -0.5823 & -0.1195 & 0.1323 \\ 0.9017 & 0.0014 & -0.1680 \end{pmatrix}$$

The agreement between the two matrices is still good.

It was then investigated what effects uniformly distributed noise had on this result. The largest difference between two readings of the $Ce^{4+}$-concentration in this time series was approximately $10^{-8}$ M, and to this was added random noise with a maximum amplitude of $10^{-12}$ M. i.e. the signal to noise ratio was approximately $10^4$. The average result for the Jacobian matrix from ten different runs was

$$\mathbf{J} = \begin{pmatrix} -0.1326 & -0.0740 & -0.0000 \\ -0.5818 & -0.1196 & 0.1326 \\ 0.9013 & 0.0015 & -0.1684 \end{pmatrix}$$

This result is still quite satisfying, but decreasing the signal to noise ratio further will cause the results to deteriorate. As an example we consider the average of ten different runs with the signal to noise ratio decreased to 2000. Then we get the result

$$\mathbf{J} = \begin{pmatrix} -0.1513 & -0.0744 & -0.0036 \\ -0.6383 & -0.1205 & 0.1204 \\ 0.9336 & 0.0025 & -0.1519 \end{pmatrix}$$

Thus it would appear that a signal to noise ratio of $10^4$ or more is desirable in order to get satisfactory results.

This looks a little discouraging for the prospect of getting satisfactory experimental results, but some of the explanation might be found in the relative stiffness of the Oregonator. The third eigenvalue of the Jacobian matrix is -0.41, which is the main factor in the determination of the sampling interval. One could suspect that a numerically smaller third eigenvalue would lead to greater tolerance of noise.

We now assume that the sampling interval, $\Delta t$ has been selected, and we focus on the fastest of the three modes. The eigenvalue of this mode, $\lambda$, is the inverse of the characteristic time, $\tau$, of the system, which in turn must be approximately equal to $\Delta t$ to get the best determination of the $a$ and $b$-coefficients. To sum it up, it means that

$$\frac{1}{-\lambda} \;=\; \tau \;\approx\; \Delta\, t$$

We now turn our attention to the determination of $e^{\lambda\Delta t}$. This comes from the linear determination of the $a$ and $b$-coefficients. We can therefore imagine that $e^{\lambda\Delta t}$ can be determined as the inclination between two measurements, $S$, separated by $\Delta t$, i.e. $\frac{\Delta S}{\Delta t} \approx e^{\lambda\Delta t} \approx e^{-1}$. We then get

$$\Delta S \approx e^{-1}\Delta t \approx \frac{1}{-e\lambda}$$

For a given experimental setup it is possible to determine a maximum noise amplitude, $\delta S$, on the measurements. This will be more or less constant from experiment to experiment with the same equipment. Thus we get for the signal to noise ratio

$$\frac{\Delta S}{\delta S} \;\propto\; \frac{1}{-\lambda}$$

Assume now that for a given experimental setup and eigenvalue, $\delta S$ has been brought down to give an acceptable determination of the eigenvalue. Imagine that we were able to change the eigenvalue without changing anything else in the system, then we can conclude that if the eigenvalue was smaller numerically, $\delta S$ remaining constant, the relative error on $\lambda$ would be smaller.

These are by no means rigorous arguments, but they do justify the hope for more tolerance of noise in less stiff systems.

### 6.3.3 How to Get Correct Results

In this section we consider the results from Kinetic Spectrometry and which precautions that should be taken to get correct results. It is evident that some features of the method do not apply as easily as on the computer.

One major concern is the problem of applying perturbations with the correct amount of perturbation species. First of all it is necessary to make sure that the perturbation burette contains the correct concentration of species. To avoid problems, freshly produced solutions should be used, and if light promotes decomposition of the perturbation species, e.g. $Ce^{4+}$, the perturbation burette should be covered with non-transparent material. Also, to

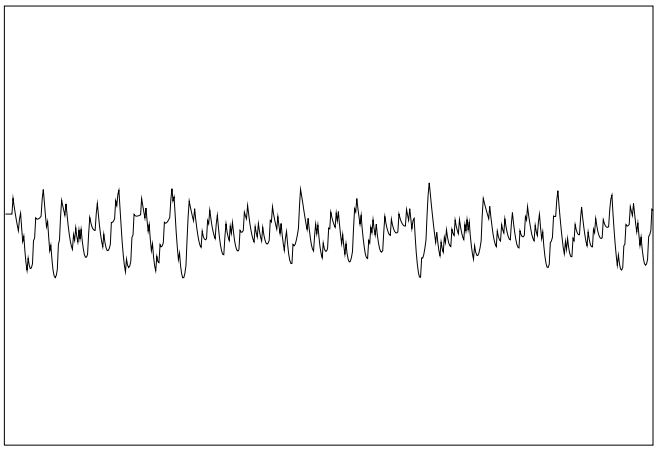

**Figure 6.3**: A time series showing the $Ce^{4+}$-oscillations around the stable stationary state, when applying Kinetic Spectrometry to the Oregonator.

make sure that the first few additions of the perturbation species was not in fact a mixture of cell-solution and perturbation-solution, due to diffusion between the cell and the tube from the burette, the tube was connected with the cell, and after the system had returned to the stationary state, a single large perturbation was applied. This, in part to verify that the system did indeed perform damped oscillations towards the stationary state, made sure that the content of the tube was the correct compound. After the system had returned to the stationary state, the experiment was started.

Having solved that problem, one also has to make sure that the correct volume of solution is applied from the perturbation burette. The main problem in this connection is friction between the burette piston and the sides of the burette. Because we want to avoid too much dilution when perturbing, the perturbation volume should be small. This means that the piston should only move a little on each perturbation. If the friction is too high, the risk is that the piston will not move the first couple of times it was supposed to, but instead moves the third or fourth time and thus makes the results unreliable. In these experiments, the piston of the perturbation burette was therefore polished down, so that it slid easily through the burette but at the same held tight. This should minimize the error.

As it turned out, the most difficult problem was one not even considered at the beginning of the experiments. As described earlier, the system is in a stable stationary state at the start of the perturbations. Consider the time series in figure 6.3, where perturbations are applied to the Oregonator. After starting the perturbations, the system oscillates around the stable stationary state. It can be observed that the mean $Ce^{4+}$-concentration is more or less constant throughout the time series. Thus we would expect to be able to observe the same in experiments.

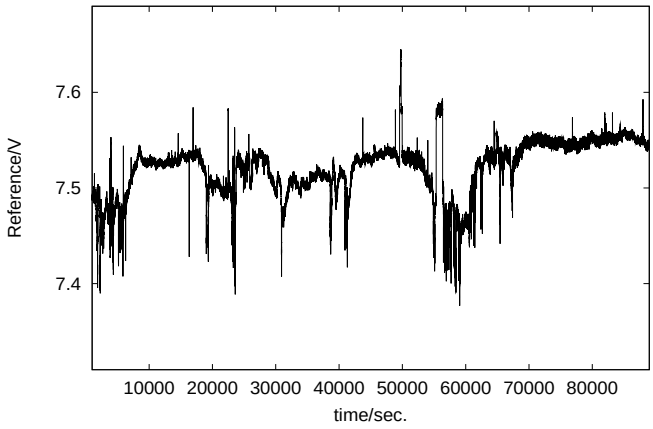


**Figure 6.4**: A typical run showing the lamp output. The measured signal is the current from an external circuit amplified by the diode-transistor. The amplification depends on the light intensity on the transistor.

The critical condition for being able to do so is the presence of an absolutely stable stationary state. In order for the stable stationary state to appear stationary, the output from the lamp must be constant. Otherwise, the measurements with the photomultiplier will not be constant. To find out whether this was the case or not, the lamp output was measured separately with the diode-transistor. The result from a typical run over a little more than 24 hours can be seen in figure 6.4. It is evident that the lamp output is nowhere near being constant. The purpose of the reference measurements was consequently to correct the absorption measurements by incorporating the fluctuations of the lamp in the corrected measurement. For this purpose, the voltage on the lamp was varied slightly in the area where measurements were made. This was done at a time where the system was almost certainly in a stable stationary state. The following connection was found at one time:

$$m = -0.0933\text{V} + 0.0239r$$

$m$ is the measurement and $r$ the reference. These numbers were calculated from points located around the values of the reference during an experiment. The calculated numbers were of course critically dependent of the geometry of the experimental setup, and a small change in the geometry would lead to a small change in the expression. The corrected measurement was therefore calculated as $(m + 0.0933\text{V})/r$. This will produce the minimal error on the corrected signal. Say that there was a small error in the determination of the value -0.0933 V in the calibration so that it could only be said to be somewhere in the interval [-0.0953:-0.0913] V. Then the error on the corrected measurement, assuming that the reference fluctuates between 7.4 V and 7.6 V, would be $\frac{0.04}{7.4} - \frac{0.04}{7.6} = 0.06\%$. During an experiment, the fluctuation of the reference would be much less (cf. the last part of fig. 6.4).

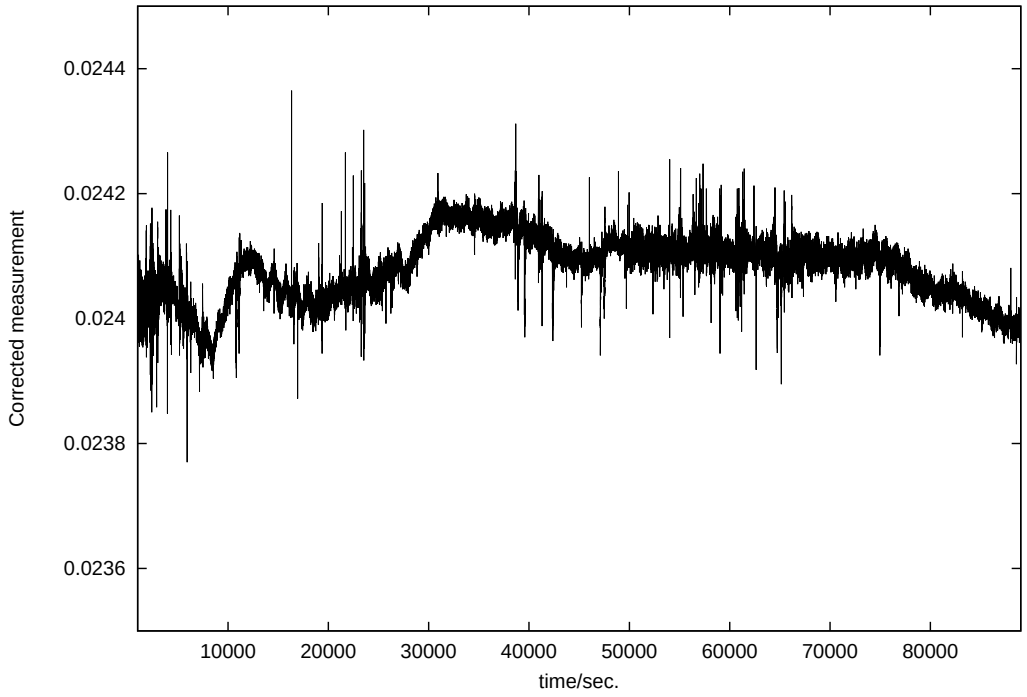


**Figure 6.5**: The corrected measurements from the time series recorded simultaneously with the reference in fig. 6.4. The last half of the time series or more was expected to be a stationary state.

Consider the time series in fig. 6.5. It shows the evolution of the corrected measurement simultaneously with the reference of fig. 6.4. At least the last half of this time series was expected to show a stable stationary state. Obviously, this is not the case. The time series in fig. 6.5 is not unique. On the contrary. We therefore have to ask ourselves the question: Did we actually have a stable stationary state? It should be mentioned that even though the calibration expression might not have been completely correct, it should still reveal whether the system was in a stationary state or not.

The equipment used in these experiments, including flow burettes, was the same as in the quenching experiments [27]. The flow provided from the burettes was adequate for the quenching experiments, but was most likely not constant enough for these experiments. This leads to one conclusion on how to get correct results in Kinetic Spectrometry: One has to achieve a completely steady flow of reactants. One way of accomplishing this could be to use smaller flow burettes than in these experiments run at a correspondingly faster rate to get the same overall specific flow rate. This concern was the main reason for changing from the slow to the fast flow rate.

In this connection it should be mentioned that the light sensitivity of the reaction should also be taken into account. Although not as sensitive to light as the ruthenium-catalyzed version, it was found that the Ce-catalyzed BZ reaction is indeed sensitive to light, and consequently the stationary state achieved in an experiment is sensitive to the amount of light around the experimental setup. The setup should therefore be shielded against any exterior light sources, which was attempted as much as possible in these experiments.

To sum up on this section, the precautions concerning the perturbation burette should be followed. It would be a good idea also to invest in a lamp with a steady output to avoid having to make reference measurements and consequently having to determine the relation between reference measurements and measurements of the stable stationary state. Furthermore the experimental setup should be shielded from external light sources. If concerned about the influence of the measurement lamp on the chemistry, measurements of electrode potentials could be used instead of absorption measurements. Finally, the importance of getting a steady flow can not be overestimated.

### 6.3.4 Results

The Kinetic Spectrometry experiments were successful in finding an eigenvalue pattern similar to the one found for the Oregonator in section 6.2.5. The attempt to determine a credible Jacobian matrix, however, was unsuccessful.

To convince ourselves that the system undergoes a Hopf bifurcation when lowering the bromate concentration from the value used in the quenching experiments, a crude investigation of the square of the amplitude of the oscillations as a function of the bromate-flow concentration was made. The result can be viewed in figure 6.6. It shows that lowering the bromate concentration is equivalent to lowering the specific flow rate, which was shown [12] to make the system undergo a Hopf bifurcation. It should be mentioned that at bromate-flow concentration 0.030 M there are no oscillations, and damped oscillations back toward the stationary state decay very slowly. This corresponds well with the intersection with the x-axis in fig. 6.6.

Thus having determined the system to be located close to a Hopf bifurcation on the stable side at both the high and low flow rates, we can investigate the results. For both the low and high flow rates a $\Delta t$ of 8 s was chosen. The results for the eigenvalues in two, three, and four dimensions for the eigenvalues of the Jacobian matrix were in one experiment at the low flow

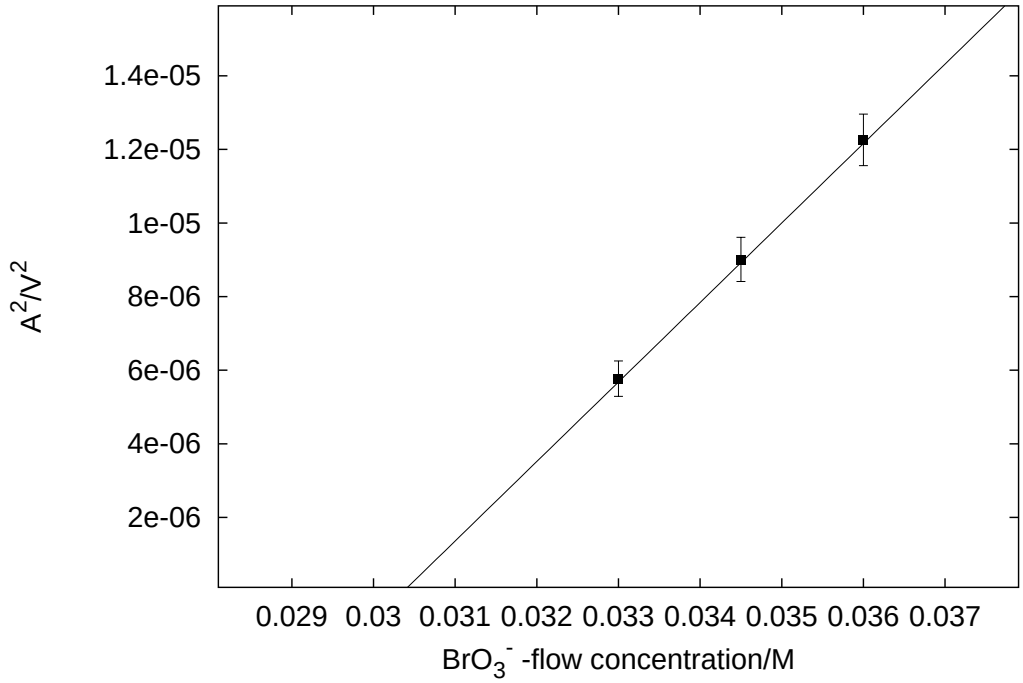


**Figure 6.6**: The square of the uncorrected amplitude, A, as a function of the bromate-flow concentration.

rate:

$$\begin{aligned}(\rho_1, \rho_2) &= (-0.130 + i0.778, -0.130 - i0.778)\\ (\rho_1, \rho_2, \rho_3) &= (-0.250 + i0.828, -0.250 - i0.828, 0.624)\\ (\rho_1, \rho_2, \rho_3, \rho_4) &= (-0.202 + i0.827, -0.202 - i0.827, 0.756, -0.323)\end{aligned}$$

These results were obtained by perturbing with $Ce^{4+}$. At the high flow rate, the corresponding results from one experiment were:

$$\begin{aligned}(\rho_1, \rho_2) &= (0.168 + i0.321, 0.168 - i0.321)\\ (\rho_1, \rho_2, \rho_3) &= (-0.228 + i0.671, -0.228 - i0.671, 0.796)\\ (\rho_1, \rho_2, \rho_3, \rho_4) &= (-0.177 + i0.736, -0.177 - i0.736, 0.853, -0.227)\end{aligned}$$

These results were obtained by perturbing with $Br^-$. *From these results we conclude*, in accordance with the pattern of results from section 6.2.5, *that the system has three slow modes*. One should notice the imaginary parts of the complex eigenvalues in three dimensions. For both flow rates they correspond very well with the period of the damped oscillations. This was the main factor in choosing $\Delta t = 8$ s. Although these results might look

encouraging, it was neither possible to reproduce them with a satisfactory accuracy from one $Ce^{4+}$-experiment to the next nor from the $Ce^{4+}$ to $Br^{-}$-experiments. The main reasons for this are described in the previous section. If it is not possible to reproduce the $a$-coefficients from one experiment to the next it is impossible to obtain a credible Jacobian matrix, because the theory predicts equal $a$-coefficients for each experiment, which was also found in the computer simulations. It also implies that the $b$-coefficients were not determined correctly either. The irreproducibility meant that experiments with perturbations of $HBrO_2$ were not even tried.

The main result is therefore that *a three-dimensional description of the BZ reaction is adequate*, at least for the conditions applied in these experiments. One might be concerned whether there was too much noise to make this conclusion, but the reproducibility was good enough to show this pattern in several different experiments. The magnitude of the real eigenvalue in three dimensions, comparable to the real part of the complex eigenvalues, around 0.05 $s^{-1}$, also indicates a relatively small sensitivity to noise.

# 7
# Conclusions and Perspectives

The critical part of controlling a chemical system is the identification. We saw that once the identification had been performed adequately, the control worked with a large margin on the placement of the poles. It was therefore natural to ask if the identification could serve other purposes.

The answer was Kinetic Spectrometry. We have seen how it reproduces the Jacobian matrix of a dynamical system with a precision limited only by nonlinearities and noise, which can be set almost arbitrarily low on the computer. We have investigated how it extracts the maximal amount of information in cases where a full Jacobian matrix can not be obtained. Both for the slow left eigenvectors with the full dimension and, perhaps even more important, for the Jacobian matrix with a reduced number of dimensions. This Jacobian matrix has the correct eigenvalues but it is not a section of the full Jacobian matrix. However, if we want to construct a model based on this Jacobian matrix, we are not necessarily interested in writing it with elementary reactions but with the resulting rate expressions for the species used for perturbing the system. Thus we are interested in the resulting Jacobian matrix elements which is exactly what we get.

Having determined the Jacobian matrix correctly still does not reveal the chemical mechanism. It will, however, reveal whether a proposed model is true or not. If the Jacobian matrix determined from an experiment does not agree with the Jacobian matrix calculated directly from the model with the correct parameter values then the model is not correct. Alternatively, if one had confidence in the model but not in the values given for the rate constants, one could calculate the Jacobian matrix symbolically and derive

the rate constants from the experimental result.

If nothing is known about the model, the Jacobian matrix can still be used for evaluating the relations between species. Consider the Jacobian matrix calculated for the Oregonator on page 35. From the elements in the third row we can conclude that $HBrO_2$ has a positive influence on the rate of formation of $Ce^{4+}$ and that $Br^-$ has no influence on that rate. By inspection of the model in table 2.2 we can see that this is true. We can not, however, see the autocatalytic reaction of $HBrO_2$ or that the negative influence of $Br^-$ on the rate of formation of $HBrO_2$ is the sum of a positive and a negative contribution. However, the different elements may still be used as pieces in a puzzle, and we can only hope that there are enough pieces to get an impression of the full picture.

We can conclude that Kinetic Spectrometry is a powerful tool in analyzing chemical, dynamical systems. More so than the quenching method, but they should not be perceived as competitors. On the contrary. If absolutely nothing is known about an oscillating chemical reaction, the two methods may complement each other very well. Kinetic Spectrometry can only be used if one knows which species to use for perturbing the system. These can be found by trying to quench the system with different species. Once one species has been found, that species can be used for Kinetic Spectrometry which will determine the dimension of the system. Thus the number of remaining species that can be used for Kinetic Spectrometry is known. Further quenching experiments will determine which species. This option could for instance be applied on the glycolytic oscillations in living yeast cells (fig. 1.1). Little is still known about this reaction.

In light of the experimental results in this thesis, or the lack of it, one might be entitled to ask whether Kinetic Spectrometry will have any effect in analyzing real chemical systems. In this connection we notice that the irreproducibility was not worse than it was still possible to determine the number of dimensions in the Ce-catalyzed BZ reaction to be equal to three. This was done in several independent experiments with two different species. It was also explained why the results were not reproducible. If the guidelines in section 6.3.3 are followed, the method ought to be successful. The computer simulations have shown that if the experimental setup can be optimized to the requirements of the method, then the method *will* be successful. This opens a number of different possibilities. All the different reactions that have been investigated with the quenching method can also be analysed by Kinetic Spectrometry. *Any* chemical system may be analysed by Kinetic Spectrometry.

# Bibliography


[1] Belousov, B. P.; Sb. Ref. Radiats. Med. 1958; *Medgiz: Moscow* (1959).

[2] Field, R. J. and Försterling, H.-D. (1986); On the oxybromine chemistry rate constants with cerium ions in the Field-Körös-Noyes mechanism of the Belousov-Zhabotinskii reaction: the equilibrium $HBrO_2 + BrO_3^- + H^+ = 2BrO_2\cdot$ ; *J. Phys. Chem.*; **90**; 5400–7.

[3] Field, R. J., Kőrös, E., and Noyes, R. M. (1972); Oscillations in chemical systems. II. Thorough analysis of temporal oscillation in the bromate-cerium-malonic acid system.; *J. Am. Chem. Soc.*; **94**; 8649–64.

[4] Field, R. J. and Noyes, R. M. (1974); Oscillations in chemical systems. IV. Limit cycle behaviour in a model of a real chemical reaction.; *J. Chem. Phys.*; **60**; 1877–84.

[5] Gao, Y., Försterling, H.-D., Noszticzius, Z., and Meyer, B. (1994); HPLC Studies on the Organic Subset of the Oscillatory BZ Reaction. 1. Products of the $Ce^{4+}$-Malonic Acid Reaction; *J. Phys. Chem.*; **98**; 8377–80.

[6] Goodwin, G. C. and Sin, K. S.; Adaptive filtering prediction and control (Prentice-Hall, 1984).

[7] Gray, P. and Scott, S. K.; Chemical Oscillations and Instabilities; The International Series of Monographs on Chemistry (Oxford University Press, Oxford, 1990).

[8] Guckenheimer, J. and Holmes, P.; Nonlinear Oscillations, Dynamical Systems, and Bifurcations of Vector Fields; Applied mathematical sciences (Springer-Verlag New York, Inc., 1983).

[9] Hale, J. and Koçak, H.; Dynamics and Bifurcations; Texts in Applied Mathematics (Springer-Verlag New York, Inc., 1991).

[10] Hynne, F., Sørensen, P. G., and Nielsen, K. (1990); Quenching of chemical oscillations: General Theory; *J. Chem. Phys.*; **92**; 1747–57.

[11] Johnson, B. R., Scott, S. K., and Thompson, B. W. (1997); Modelling complex transient oscillations for the BZ reaction in a batch reactor; *Chaos*; **7**; 350–58.

[12] Kosek, J., Sørensen, P. G., Marek, M., and Hynne, F. (1994); Normal Form Analysis of the Belousov-Zhabotinsky Reaction Close to a Hopf Bifurcation; *J. Phys. Chem.*; **98**; 6128–35.

[13] Lee, R. C. K.; Optimal Estimation, Identification, and Control; Res. Monograph 26 (M.I.T. Press, Cambridge Massachusetts, 1964).

[14] Marsden, J. E. and McCracken, M.; The Hopf Bifurcation and Its Applications; Applied mathematical sciences (Springer-Verlag New York, Inc., 1976).

[15] Nagy, A., Sørensen, P. G., and Hynne, F. (1995); Quenching of Oscillations in the Permanganate-Hydroxylamine Reaction; *Z. Phys. Chem.*; **189**; 131–38.

[16] Ott, E., Grebogi, C., and Yorke, J. A. (1990); Controlling Chaos; *Phys. Rev. Lett.*; **64**; 1196–99.

[17] Peng, B., Petrov, V., and Showalter, K. (1991); Controlling Chemical Chaos; *J. Phys. Chem.*; **95**; 4957–59.

[18] Perko, L.; Differential Equations and Dynamical Systems; Texts in Applied Mathematics (Springer-Verlag New York, Inc., 1996); 2nd edn.

[19] Petrov, V., Crowley, M., and Showalter, K. (1994); Controlling spatiotemporal dynamics of flame fronts; *J. Chem. Phys.*; **101**; 6606–14.

[20] Petrov, V., Gáspár, V., Masere, J., and Showalter, K. (1993); Controlling chaos in the Belousov-Zhabotinsky reaction; *Nature*; **361**; 240–43.

[21] Petrov, V., Mihaliuk, E., Scott, S. K., and Showalter (1995); Stabilizing and characterizing unstable states in high-dimensional systems from time series; *Phys. Rev. E*; **51**; 3988–96.

[22] Petrov, V. and Showalter, K. (1996); Nonlinear Control of Dynamical Systems from Time Series; *Phys. Rev. Lett.*; **76**; 3312–15.

[23] Petrov, V. and Showalter, K. (1997); Nonlinear prediction, filtering, and control of chemical systems from time series; *Chaos*; **7**; 614–20.

[24] Press, W. H., Teukolsky, S. A., Vetterling, W. T., and Flannery, B. P.; Numerical Recipes in Fortran (Cambridge University Press, 1992); 2nd edn.

[25] Scott, S. K.; Chemical Chaos; The International Series of Monographs on Chemistry (Oxford University Press, Oxford, 1993).

[26] Sirimungkala, A., Försterling, H.-D., and Noszticzius, Z. (1996); HPLC Studies on the Organic Subset of the Oscillatory BZ Reaction. 2. Two Different Types of Malonyl Radicals in the $Ce^{4+}$-Malonic Acid Reaction; *J. Phys. Chem.*; **100**; 3051–55.

[27] Sørensen, P. G. and Hynne, F. (1989); Amplitudes and Phases of Small-Amplitude Belousov-Zhabotinskii Oscillations Derived from Quenching Experiments; *J. Phys. Chem*; **93**; 5467–74.

[28] Sørensen, P. G., Lorenzen, T., and Hynne, F. (1996); Quenching of Chemical Oscillations with Light; *J. Phys. Chem.*; **100**; 19192–96.

[29] Sørensen, P. G., Skødt, H., and Hynne, F.; Unpublished results.

[30] Strogatz, S. H.; Nonlinear Dynamics and Chaos (Addison-Wesley, Reading, Massachusetts, 1994).

[31] Venkataraman, B. and Sørensen, P. G. (1991); ESR Studies of the Oscillations of the Malonyl Radical in the Belousov-Zhabotinsky Reaction in a CSTR; *J. Phys. Chem.*; **95**; 5707–12.

[32] Vukojević, V., Sørensen, P. G., and Hynne, F. (1993); Quenching Analysis of the Briggs-Rauscher Reaction; *J. Phys. Chem.*; **97**; 4091–4100.

[33] Wang, J., Sørensen, P. G., and Hynne, F. (1994); Transient Period Doublings, Torus Oscillations, and Chaos in a Closed Chemical System; *J. Phys. Chem.*; **98**; 725–27.

[34] Wang, J., Sørensen, P. G., and Hynne, F. (1995); Transient Complex Oscillations in the Closed Belousov-Zhabotinsky Reaction: Experimental and Computational Studies; *Z. Phys. Chem.*; **192**; 63–76.

[35] Wilkinson, J. H.; The Algebraic Eigenvalue Problem (Clarendon Press, Oxford, 1965).

[36] Zhabotinskii, A. M. (1964); Periodic liquid-phase oxidation reactions; *Proc. Acad. Sci. USSR*; **157**; 392–5.